USF Tampa Graduate Theses and Dissertations   USF Graduate Theses and Dissertations

7-19-2005

Material Properties and Volumetric Porosity of Biomaterials for Use in Hard Tissue Replacement

Christopher G. Papangelou
University of South Florida

Follow this and additional works at: https://digitalcommons.usf.edu/etd

Part of the American Studies Commons

Scholar Commons Citation

Material Properties and Volumetric Porosity of Biomaterials for Use in Hard Tissue

Replacement

by

Christopher G. Papangelou

A thesis submitted in partial fulfillment
of the requirements for the degree of
Master of Science in Biomedical Engineering
Department of Chemical Engineering
College of Engineering
University of South Florida

Major Professor: Wesley Johnson, Ph.D.
William Lee, Ph.D.
John Wolan, Ph.D.

Date of Approval:
July 19, 2005

Keywords: bone replacement, porosity, carbon fiber reinforced epoxy, glass fiber reinforced epoxy, zirconia toughened alumina, composite

Table of Contents

List of Tables

List of Figures

Material Properties and Volumetric Porosity of Biomaterials for Use in Hard Tissue Replacement

Christopher G. Papangelou

ABSTRACT

Metal implants are a type of hard tissue replacement currently used. Metals used for implants include: stainless steel, titanium, chrome, and cobalt alloys. Such implants often fail at the interface with bone. Metal implants fail when the surface of the implant is coated with an osteoconductive material. An osteoconductive material provides scaffolding for cellular migration, cellular attachment, and cellular distribution. A reason for metal implant failure could be the vastly different material properties than bone. Motivation for the research was to find a suitable bone substitute other than metal. Materials considered were: zirconia toughened alumina, carbon fiber reinforced epoxy, and glass fiber reinforced epoxy. Those materials have been used in previous biological applications and can be cast into complex configurations.

Objectives of the study were to compare material properties of the composites to bone. A method to create porosity was then tested in the material that was similar to bone in critical material property.

Some of the materials were statistically similar to bone in yield strength. Method to create interconnected porosity in those materials resulted in 49% void space.

Chapter 1: Introduction

1.1 Background

Metal is a material used in some applications of hard tissue replacement. Metals used for implants include: stainless steel, titanium, chrome, and cobalt alloys. Metal implants often loosen at the interface with bone [42]. Metal implants fail even when the surface of the implant is coated with an osteoconductive material.

An osteoconductive environment must be established in a suitable bone replacement [40]. An osteoconductive material provides scaffolding for cellular migration, cellular attachment, and cellular distribution [23]. Bone will integrate into the osteosonductive material and secure the bone replacement. A reason for metal implant failure could be the vastly different material properties compared to bone.

Carbon fiber reinforced carbon composites are mentioned as candidate bone replacement material because of their comparable rigidity to cortical bone [24]. A comparison of bone rigidity to bone replacement material rigidity is insufficient to determine bone replacement suitability. A more detailed comparison of bone to the bone replacement material is needed to determine a suitable bone replacement. Material properties of ultimate strength, yield strength, and elastic modulus were compared between potential bone replacement materials and bone itself. Yield strength is the maximum stress in its elastic region. Ultimate strength is the maximum stress reached before failure of the material. Elastic modulus of a material is the ratio of the linear stress to the linear strain.

Motivation for the research was to find a suitable bone replacement other than metal. Materials considered were: zirconia toughened alumina (ZTA), carbon fiber reinforced

epoxy, and glass fiber reinforced epoxy (CFRE and GFRE). Those materials possess two features: 1) have been used in previous biological applications such as joint prostheses, bone plates, dental posts, and long bone replacement and [6] 2) they can be cast. Ability of the materials to be cast allows them to be fabricated into complex shapes. An understanding of the material being replaced is needed in order to choose a suitable bone substitute from those selected in this study.

1.2 Bone

Bone is a composite material. A composite material is one that consists of two or more phases that are not soluble in each other [18]. Bone consists of both an organic phase and inorganic phase [27].

Bone is a hierarchical structure. It contains different structures on different levels. At the macroscopic level bone is subdivided into two forms: cortical and trabecular [27]. Cortical bone is dense and found in long bones. Cortical bone porosity consists of Haversian canals, Volkmann's canals, resorption spaces or canals, lacunae, and canaliculi. Haversian canals contain small blood vessels and nerve fibers [28]. Haversian canals are aligned approximately along the long axis of bone [28]. Volkmann's canals perforate Haversian canals. Volkmann's canals are oriented approximately perpendicular to the long axis of the bone, connecting vascular and nerve supplies [28]. Resorption canals are formed by osteoclasts. Resorption canals are temporary spaces in the initial stage of remodeling [28]. Lacunae are small spaces, about 10 μm diameter, that house osteocytes. Osteocytes are bone cells that play a large part in signaling need for bone repair. Canaliculi are even smaller canals that form a network connecting all the lacunae together, in a given bone. Cortical bone acts as an "envelope" for trabecular bone, together providing resistance to bending, torsional, and compressive forces (Figure A.1) [27].

Trabecular bone is a highly porous form of bone. The structure of trabecular bone is a latticework of bars or struts (trabeculae) [27]. Trabeculae are struts aligned to support the

cortical shell of bone [27]. Three dimensional structure of trabecular bone consists of interconnected pores, much like a sponge, of varying sizes, 50 – 450µm.

1.3 Bone architecture

Porosity, apparent densities, and osteoconductive environment distinguish cortical and trabecular bone from one another. Cortical bone is defined as bone with less than 30% porosity (typically 5-10%) [3]. Porosity of trabecular bone is typically 50 to 90% [3]. Pore sizes range from 50- 450 µm [5]. Trabecular bone can be described architecturally as a bridging network of trabeculae forming a series of interconnected pores.

Apparent density of any solid is defined as the ratio of mass to bulk volume. Apparent density of human femoral cortical bone is in the range of 1.80 to 1.90 g/cm^3 [5]. Apparent density of femoral trabecular bone is 0.20 g/cm^3 to 0.40 g/cm^3 [5]. Those values vary depending on the physical and inherited conditions of an individual.

Osteoconductivity is described by Urist et al as a material property that supports tissue ingrowth, osteoprogenitor cell growth and development for bone formation [23]. Osteoconduction is optimized by materials that mimic both bone structure and chemistry [9]. Bone grafted from a donor is regarded to as the gold standard for bone replacement material [40]. The primary determinate of the speed and completeness of osteoincorporation is the three dimensional structure of the implant [9].

Osteoincorporation is described as the ability of bone to incorporate into the structure of a material [40]. In order to achieve osteoincorporation three elements are necessary: 1) scaffolding for osteoconduction 2) growth factors for osteoinduction 3) and progenitor cells for osteogenesis [40]. Osteoconduction is accomplished through structure similar to bone. Osteoinduction requires the proteins necessary to grow bone. Both elements are needed along with progenitor cells for osteointegration.

1.4 Bone literature

LeGeros et al claimed that porous structures with small interconnecting pores are more of a limiting factor for osteoconduction than actual pore size [23]. LeGeros et al noted importance of pore size and interconnectivity as critical factors affecting diffusion of nutrients, cell attachment, cell migration, and cell expression that are vital for bone formation [23]. However, there is no consensus as to which pore size, shape, or interconnection promotes the best osteoconduction.

Vaccaro suggested that the combination of an osteoconductive matrix, an osteoinductive growth factor, and osteogenic cells may surpass the importance of graft material used [40]. According to Vaccaro, any non toxic material can be used as long as it has an osteoconductive matrix, an osteoinductive growth factor, and osteogenic cells. Composite grafts were tested for this study. Composite materials are used for the ability to tailor mechanical properties and light weight.

1.5 Composite materials

A composite material is one that consists of two or more constituents that are not soluble in each other [18]. One of these constituents is referred to as the reinforcing phase, and the other constituent, in which it is embedded, is the matrix phase [18]. The reinforcing phase is generally found in the form of fibers, particles, or flakes [18]. Composite materials are used in many applications because of the high strength, toughness, and low weight. Strength of a material is defined as the applied load (force) point at which the material yields or fails [28]. Toughness of a material is (MPa-m$^{1/2}$) the amount of resistance to crack growth.

Particle and fiber based composites were used in this study. Particle based composites have hard particles surrounded by a softer matrix. Particle diameter is often only a few microns in diameter and comprises about 20 to 40 percent volume of the composite. Particle reinforced composites have a large volume fraction of particle dispersed in the

matrix. Load is shared by particles and the matrix. In the case of ZTA, fine zirconia particles are uniformly dispersed in an alumina matrix [32]. Zirconia particles expand during firing and stress the alumina matrix, causing microcracks [32]. Toughening is due to more energy required for crack growth around the higher elastic modulus zirconia particles.

Reinforcing fibers are made from short (discontinuous) or long (continuous) fibers [18]. Fiber reinforced epoxy was used in this study. Viscosity and flow rate can be adjusted in epoxy. Low viscosity epoxy allows wetting of the reinforcing phase and adhesion [18]. Fibers increase the elastic modulus of the matrix material [18]. Increase in elastic modulus is due to the strong covalent bonds of the fibers to the matrix material. Strong covalent bonds increase the elastic modulus because bonds must be broken or moved to break or extend the fiber [18]. The material properties of composite materials can be sufficient to mimic bone material properties. However, the main barrier in using composites as bone replacements is creating an optimal osteoconductive scaffold [40].

1.6 Creating a porous network (epoxy)

Polymers are macromolecules consisting of different monomer length chains. Polymers are either formed by a chain-reaction polymerization or a step-reaction polymerization [14]. Chain-reaction polymerization requires an initiator to start the expansion of the reaction [14]. Once the reaction is initiated, the monomers link together to form a long chain (Figure A.2). A reaction can be initiated by a free radical, denoted as R in Figure 8. Different chain lengths give the polymer different molecular weights and consequently different properties. Those properties include resistance to chemicals, mechanical properties, melting point, and dissolution in specific solvents. A step-reaction polymerization, or condensation reaction, involves polymer chains growing by reactions that occur between two molecular species [14].

Current methods to create an interconnected porous network from polymeric materials for this research did not meet the desired end product requirements. Those requirements

were: to create and have the ability to control the volumetric arrangement of porosity, not use any toxic substances. Ability to control volumetric arrangement of porosity can produce a configuration of the pores in a gradient similar to bone. A gradient of pores will promote and direct bone growth in the selected materials. Current methods used for creating porosity in a thermosetting polymer (epoxy) include gas nucleation, gas foaming (blowing), and phase separation (emulsion). Those methods produce closed or open cell matrices. Closed cell matrix is void spaces within the material that are not interconnected. Interconnected pores depict open cell matrices. Closed cell techniques were not considered in this research.

Method of gas nucleation consists of a two step procedure [19]. The first step saturates the polymer with non-reactive gas at elevated pressures [19]. The supersaturated polymer is heated to near glass transition temperature, T_g, to induce the growth of gas bubbles [19]. The method of gas nucleation was not considered because it does not allow control of the volumetric arrangement of the porous area within the material.

Method of gas foaming is the most commonly used method to produce macroporous foams with interconnected pores [19,38]. A macroporous foam has pore sizes of 50 nm or larger. It does not allow control of the volumetric arrangement of the porous area within the material.

Phase separation techniques also produce interconnected pores [19, 20, 26, 27]. Researchers encounter the same inability to control volumetric arrangement of pores with phase separation techniques as discussed with the method of blowing. Researchers do not have control of volumetric arrangement of the pores within the substrate material. Phase separation also was not considered because construction of a desired 3 dimensional interconnected porous network structure requires more than a one step process. Some phase separation techniques also require the use of toxic substances.

The inability to control the volumetric arrangement of porous area within the material and the use of toxic substances led me to investigate methods to create tailored structures

6

that can imbed in a substrate material. The tailored structure can then be exposed at the surface after it has cured. The tailored structure then could be dissolved from the substrate material using non-toxic solvents such as water. Removal of the tailored structure would leave an interconnected porous material.

1.7 Creating a porous network (dissolvable polymers)

Non-toxic methods for creating porosity with dissolvable polymers such as poly(L-lactic acid) (PLLA), poly(L-lactic-co-glycolic acid) (PLGA), poly(glycolic acid) (PGA), and poly(vinyl alcohol) (PVA) were considered. Consideration was based on their current use in biological applications. Each of the polymers mentioned has been used in applications such as contact lenses, time released drug delivery, and dissolvable sutures. Methods for producing a porous dissolvable polymer scaffold include: PGA non-woven mesh (fiber bonding), solvent casting/particulate-leaching, phase separation (emulsion), gas foaming (blowing) [29, 30]. The method of phase separation and gas foaming was discussed in the previous section on epoxy and will not be further discussed.

Fiber bonding was one of the earliest designs in tissue engineering to create volumetric porosity. One of the first developed techniques by Mikos et al, consisted of immersing PGA fibers in a PLLA solution [29]. The method was used to produce foam with porosities as high as 81% [29]. Fiber bonding process was rejected because it requires undesirable use of toxic solvents to achieve a PLLA solution [29].

Solvent casting/particulate-leaching involves mixing solid particles, such as sodium chloride, with a polymer solution and casting the mixture in a desired shape [41]. Sodium chloride is dissolved from the mixture with water to produce a porous structure [41]. Pore size and network extent are dependent on the sodium chloride particle size and weight fraction [41]. Seventy weight percent and above of sodium chloride particles results in pores of high interconnectivity [41]. Solvent casting/particulate-leaching method requires using undesired organic solvents and strong acids to attain a polymer solution.

1.8 Polymers

PVA was used in the method to create porosity in epoxy. PVA is a water soluble polymer of low toxicity. PVA is made up of repeating alcohol and acetate units.   PVA is also available with different molecular weights of the parent poly vinyl acetate and different percent hydrolysis. Dissolution rate of polyvinyl alcohol in water varies accordingly. As the percent hydrolysis of the polymer increases, (increase in the alcoholic groups, decrease in the acetate groups), the temperature required to dissolve the polymer increases.

Epoxy is a thermosetting polymer that cures when mixed with a hardening agent. Thermoset polymers have covalent bonds linking the polymer chains [18]. Thermosets are insoluble in warm saline after cured [18].

Chapter 2: Methods

2.1 Beam testing

Four simple beams were fabricated from polyethylene stock. Polyethylene beams were used as master positives for molding. Polyethylene beams were two different thicknesses (6.5 mm, 5.5 mm) (Figure A.3). Lengths of the beams were chosen to be three inches. A box (Figure A.4), used to cast the polyethylene beams, was fabricated from a 0.25 in thick board of wood. The box was made out of two halves. Each half was held together by epoxy. Once constructed, each half of the box was coated with epoxy on the inside portion. Silicone rubber molding material was mixed in the appropriate manner as specified by the manufacturer (Polytek silicone rubber, Easton, PA). Mixed silicone rubber was placed in half of the box. Each polyethylene beam was coated with release agent. Four polyethylene beams were then cast half submerged into silicone rubber. One end of the beam was pressed against the side of the box to create a hole in the silicone rubber. The hole was used to pour the selected materials into the mold. Once this half of the silicone rubber was cured (24 hours), more silicone rubber was mixed and poured into the second half of the box. The cured half of the box containing the silicone rubber and polyethylene beams was flipped over and placed on the second half of the wooden box. Rubber bands were placed around the box to keep the two halves properly aligned. Rubber bands were removed and the two halves of the box were separated after 24 hours. Polyethylene master positives were removed leaving negative cavities for fabrication of the selected material beams (CFRE, GFRE, ZTA).

Beams were constructed of three different composites. Each composite set consisted of three different percentages of reinforcing phase amounts. GFRE and CFRE beams consisted of 1, 5, and 10 volume percent for each of the respective reinforcing fibers. Carbon fibers were 7.2 microns in diameter and 6 mm long (Fortafil 160 chopped carbon, Rockwood, TN). Chopped S-2 glass fibers were 7-13 microns in diameter and 6.4 mm long (Advanced Glassfiber Yarns, LLC, Aiken, SC). Percentage of material reinforcement was computed from the known density of each material and the equation:

$$Volume = mass / density \qquad (1)$$

Specific gravity values of the epoxy were as follows: specific gravity of the resin- 1.10 g/mL and specific gravity of the hardener- 1.00 g/mL. Specific gravity values were assumed to be taken at one atmosphere of pressure. Specific gravity values can then be used as density values. Density of the chopped carbon fibers was 1.8 g/cm^3. Glass fiber density was 2.46 g/cm^3. Values used in all calculations were as specified by the manufacturers.

The ZTA was mixed with 10, 20, and 30 weight percent of 3 mol% yttria stabilized zirconia powder (Inframat Advanced Materials, Farmington, CT). Percent reinforcement for ceramic beams was done by weight percentage and the equation:

$$Weight\ of\ reinforcement\ /Total\ weight\ X\ 100 \qquad (2)$$

Ceramic beams were allowed to dry for two weeks in the laboratory environment (75ºF, 50% humidity) and fired to a temperature of approximately 2450ºF.

Beams were tested for flexural mechanical properties using a three point flexural test on an MTS® (858 Mini Bionix, Eden Prairie, Minnesota) machine. The custom three point bending apparatus (Figure A.5) was manufactured to perform beam flexural test. Mechanical properties derived from the three point bending test were: flexural yield

strength; ultimate strength; and elastic modulus. Support span of the three point bending apparatus was 43 mm and the center bending post speed was 2 mm/min.

Data was collected at a rate of ten data points per second. Acquired data were analyzed in MS Excel. Force vs. displacement plots were produced from the acquired data using MS Excel. Plots of force vs. displacement were subjected to linear regression between the linear elastic region of the plot. Linear elastic region of the plot was determined by visual inspection. Linear regression was used to derive the slope ($\Delta P/\Delta x$) used in the material property equations (Table B.1). Obtained force vs. displacement curves (Figure A.6) from the data were used for selecting the force values in the material properties calculations (Figure A.7). Ultimate stress (σ_u), yield stress (σ_y), and modulus (E) were calculated with the following equations [36]:

$$\sigma_u = 3PL/2bh^2; \tag{3}$$

$$\sigma_y = 3PL/2bh^2; \tag{4}$$

$$E = (\Delta P/\Delta x)(L^3/4bh^3), \tag{5}$$

where σ_u is the ultimate stress (MPa), σ_y is the yield stress (MPa), E is the modulus (GPa), P is the maximum flexural load (N) for the ultimate stress equation and yield load for the yield stress equation, $\Delta P/\Delta x$ is the slope of the initial linear section of the load displacement curve (stiffness in N/mm), L is the support span (mm), b and h are the width and thickness of the sample (mm).

Two beam thicknesses of each material were fabricated to compare the modulus of those two thicknesses. Comparing the modulus between the different thickness beams allows assurance that the method of manufacturing was consistent. Modulus of a material should be the same regardless of the thickness of the beam. If the modulus between beam thicknesses was statistically different they were separated into different materials.

2.2 Fiber orientation

Fiber orientations in the fiber reinforced epoxy beams were also approximated to better understand mechanical properties of the composite materials and the effect method of manufacturing has on the fiber orientation of the beams. The first method of manufacturing beams was simply pouring the mixed composite into a closed mold and was used for the 1, 5 vol% GFRE, and the 1 vol% CFRE. The second method of manufacturing beams was opening the mold, and pressing the mixed composite into each half of the mold. Those two halves were pressed together and held by a rubber band. The second method was used for the 10 vol% GFRE, 5 and 10 vol% CFRE beams.

Six specimens of the GFRE beams from the two different methods of manufacturing beams were x-rayed (20 kV, 10 seconds, Faxitron MX-20, Wheeling, IL) (Figure A.8, Figure A.9). A transparency with a protractor image was held to the monitor screen and fiber orientations, in degrees, were recorded to the nearest 10 degrees. Percentage of total fibers in a specific fiber orientation was estimated by visual inspection for each bundle of fibers within every beam. Maximum percentage of total fibers in a specific orientation for each inspected beam was then plotted against the corresponding ultimate stress value for that beam to see if a correlation existed. Correlation was assessed using the slope of linear regression and the R^2 (correlation coefficient) value.

Two methods of fabrication were used for carbon and glass fiber reinforced epoxy beams. Two methods were necessary because at high volumetric ratios (10%) of fiber to epoxy, mixture consistency did not allow pouring into the mold. 1 vol% GFRE, 5 vol% GFRE, and 5 vol% CFRE mixtures flowed well and were easily poured into the mold. The 10 vol% GFRE, 5 vol% CFRE, and 10 vol% CFRE mixtures had a thick consistency and could not be poured into the mold.

2.3 Porosity

A method to construct direct volumetric distribution of interconnected porosity in epoxy.
Testing was done using epoxy (635 thin epoxy resin, 2:1 slow hardener, US Composites,
West Palm Beach, FL) with no reinforcing components was investigated. Method to
create porosity was not used on ZTA because it did not have adequate material properties
to be considered for a bone replacement.

Method to create porosity was a variation of a method reported by Liao et al [25]. Liao et
al discuss creating a porous biodegradable polymer scaffold using a solvent
merging/particulate leaching method [25]. The process begins by sieving the granular
PLGA and sodium chloride particles to a particle size between 250-470 μm [25]. Both of
the particle species were then dry mixed together in different weight proportions [25].
Ten grams of the combination were cast into a circular-cyclindrical Teflon© mold, 20mm
in diameter and 60mm in height [25]. The bottom of the mold was a stainless steel 180
μm mesh to contain the particle matter [25]. Ten milliliters of organic solvent was then
introduced to the mixture for 30 seconds. The solvent began to dissolve the surface of
the PLGA particles [25]. A vacuum pump was then attached to the apparatus to remove
surplus solvent and coagulate the partially dissolved PLGA [25]. One hundred milliliters
of non-solvent was then passed through the composite to solidify and precipitate the
PLGA [25]. One thousand milliliters of distilled water was finally passed through the
matrix under the same vacuum and the sodium chloride particles were dissolved out [25].
Resulting samples were then dried under a 0.05 torr vacuum for 12 hours [25]. Scanning
electron microscopy, SEM, revealed a uniform pore distribution and well interconnected
structure with a porosity of $87.7 \pm 5.6\%$ and pore sizes of 343 ± 126 μm [25]. The
process displayed potential for creating and controlling porous volumetric arrangement
and pore size.

The process used in this study to create the poly (vinyl alcohol) (PVA) structure
imbedded in epoxy is different from the process used by Liao et al [25]. PVA was
chosen rather than PLGA to create porosity in the materials for its fast dissolving rate.

No sodium chloride was used in the research to create the pores in the polymer. A mild phosphoric acid was used rather than an organic solvent. Organic solvent does not dissolve PVA. Residual organic solvent is not desired for biological applications. Complete process used to create volumetric porosity in this research is further discussed in the methods section.

Process flow chart for the method used to create interconnected porosity in epoxy is displayed in Figure A.10. 0.96g of PVA granules were placed in a 25.4mm cylindrical plastic container 25.4mm in depth. PVA granules used were 125,000 molecular weight and 88 mole % hydrolyzed (Polysciences, Inc., Warrington, PA). Twenty drops of mild phosphoric acid compound, 5-6% phosphoric acid and 94-95% distilled water, wet the PVA granules. The PVA granules then adsorbed the mild phosphoric acid for five minutes. A 26mm circular plastic separator, cut from a polyethylene sheet, was placed over the PVA granules. A 100g weight was gently placed into the plastic container with the PVA granules. The weight remained on the PVA granules for 2 minutes to increase the area of PVA granules merged.

PVA construct was allowed to dry for 24 hours before it was removed from the plastic container. Twenty four hour duration of time allowed the PVA granules to dry, shrink, and merge, resulting in a porous construct of merged PVA granules (Figure A.11A). The dried PVA construct was then removed from the plastic cup. The plastic cup was coated with release agent. The PVA construct was then placed back into the plastic cup. Mixed epoxy resin and hardener was poured over the PVA to fill the plastic container. The plastic container was then placed in a vacuum chamber under a 23 in hg vacuum for approximately 5 minutes.

After 48 hours curing time, the epoxy/PVA disc (Figure A.11B) was removed from the cup by percussion. In order to expose the PVA granules to the surface of the disc, the epoxy/PVA disc was sanded using 100 and 220 grit sandpaper sequentially in figure 8 motions. Epoxy/PVA disc was finally wet sanded with 600 grit sandpaper to achieve a smooth surface (Figure A.11C). Epoxy/PVA disc was next placed in warm water to

dissolution the PVA from the disc. Water temperature was above the required temperature to dissolution PVA, 85º C, but below the T_g^o of the epoxy, 150-170ºC. Dissolution of the PVA was done in warm water for 5-7 hours with periodic stirring of the water.

2.4 Porosity estimation

Stereology was used to estimate porosity [28]. Stereology is a method of measuring three-dimensional space when only one or two dimensional measurements are available [28]. The epoxy disc was placed under a microscope. Measurements were made using a 13 mm line printed on a transparency. The 13 mm line was placed on the epoxy disc so that it was within the porous area. A microscope (16x) was used to view the portion of line that laid on void space. Void length measurements were then acquired using a digital vernier caliper (Mitutoyo, Japan). The procedure was repeated for six randomly placed lines on the specimen. Those measurements were then averaged. Equation for porosity estimation was:

$$\text{Porosity} = L_v/L_t, \tag{5}$$

where L_v is amount of length that falls over void space and L_t is entire length of the line.

2.5 Data analysis

T test were performed to statistically determine whether the mean values for the modulus of elasticity, modulus, were significantly different between the composite beam thicknesses (6.5mm, 5.5mm). Values found to be significantly different were treated as different materials and run in all the statistics. T test were then performed comparing the composite materials mean value of modulus to the modulus of bone. A 14.7 GPa modulus for bone was used for all statistics [28].

Ultimate and yield stress statistics were performed using a t test statistical analysis. Each composite material mean stress value was compared to bone. A 208 MPa ultimate stress and 100 MPa yield strength was used from literature [21, 28]. A 100 MPa yield stress was a mean value and has a range of 50-150 MPa [28]. Null hypothesis for all statistical tests was: H_o: $\mu_1 = \mu_2$. If the test statistic was smaller than the t critical value, then we reject the null hypothesis. Alternate hypothesis was: H_A: $\mu_1 \neq \mu_2$.

Chapter 3: Results

3.1 Thickness differences

30 wt% ZTA beams were significantly different for mean modulus between thick beams (*M*=3.21, *SD*=.71) and thin beams (*M*=4.29, *SD*=.88), t(6)=2.26. Two beam thicknesses within the 30 wt% ZTA were treated as different materials.

CFRE beams mean moduli were statistically similar between thick beams and thin beams for all volume percentage of carbon fiber reinforcements. GFRE beams mean moduli were statistically similar between thick beams and thin beams for all volume percentage of glass fiber reinforcements.

3.2 Modulus

Modulus of bone was significantly different than all of the tested material groups (Figure A.12, Figure A.13, Figure A.14).   Modulus for CFRE and GFRE beams increased with larger volume percent reinforcement. However, the largest mean modulus for ceramic beams was for 20 wt% ZTA (*M*=12.55, *SD*=3.94). Smallest modulus for the ceramic beams was thin 30 wt% ZTA (*M*=8.46, *SD*=.70).

3.3 Yield strength

Two of the materials selected (CFRE and GFRE) for this study had statistically similar mean yield strength to bone. (Figure A.15, Figure A.16, Figure A.17). The 10 vol% CFRE had the highest mean yield strength (*M*=119.26, *SD*=14.37) and was

statistically similar to bone mean yield strength (*M*=100, *SD*=54.77), t(6)=2.57. The 5 vol% CFRE (*M*=80.57, *SD*=17.43) also was statistically similar to bone yield strength.

Two of the different volume percentage groups of glass fiber reinforced epoxy were statistically similar to mean bone yield strength. The 10 vol% GFRE (*M*=88.11, *SD*=13.28) was the highest of the two groups. The 5 vol% GFRE (*M*=68.59, *SD*=7.52) also was statistically similar to bone yield strength.

Mean yield stress increased with larger percent reinforcement in the CFRE and GFRE beams. However, mean yield stress decreased with increasing percent reinforcement in the ZTA beams. The lowest mean yield stress was thin 30 wt% ZTA (M=5.16, *SD*=3.02).

3.4 Ultimate stress

Ultimate stress of bone was significantly different than all of the tested material groups (Figure A.18, Figure A.19, Figure A.20). Material with the highest mean ultimate stress value was 10 vol% CFRE beams (*M*=141.76, *SD*=17.4). Material with the lowest mean ultimate stress value was thin 30 wt% ZTA (*M*=8.46, *SD*=.7).

Mean ultimate stress had a similar pattern to mean modulus in the different materials. Mean ultimate stress increased with larger percent reinforcement in the CFRE and GFRE beams. However, the largest mean ultimate stress for ceramic beams was 20 wt% ZTA (*M*=12.55, *SD*=3.94). Smallest mean ultimate stress for the ceramic beams was thin 30 wt% ZTA (*M*=9.96, *SD*=.7).

3.5 Fiber orientation

Fiber orientation in the 1 vol% GFRE beams was largest in the range of 70-110 degrees (Figure A.21, Figure A.22, Figure A.23, Figure A.24, Figure A.25, Figure A.26) from the horizontal axis. A -0.03 linear regression slope indicates no correlation between fiber

orientation and ultimate stress (Figure A.27). A 0.008 correlation coefficient indicates that the linear regression line does not represent the data points. The method used to fabricate the 1 vol% GFRE, 5 vol% GFRE, and 1 vol% CFRE beams then show a tendency for the fibers to align in 70-110 degree range.

Fiber orientation of the 10 vol% GFRE was largest in the length wise direction of the beams (Figure A.28, Figure A.29, Figure A.30, Figure A.31, Figure A.32, Figure A.33). Majority of the fibers were in the zero degree orientation. There was no correlation between fiber orientation and ultimate stress (Figure A.34). Method of manufacturing the 5 vol% GFRE beams, 10 vol% GFRE, 5 vol% CFRE beams, and 10 vol% CFRE beams then show a tendency for the fibers to align zero degrees, or along the lengthwise axis of the beams.

3.6 Porosity

Method used to create porosity produced a highly interconnected porous structure in the epoxy disc (Figure A.35). Those pores were representative of the PVA structure dissolved out. PVA particles were well merged (Figure A.36) and consequently easily dissolved out. Merging also made for a highly interconnected pore structure. Porosity line test revealed the structure to be 49 % void space (Table 2). Largest pore was 3.1 mm in length. The smallest pore was 0.21 mm in length. Those values were representative of the PVA granule size used in this study.

Chapter 4: Discussion

4.1 Conclusions

Determining an acceptable material to use as a bone replacement requires the consideration of several factors. Material properties of the bone substitute need to be sufficient enough to withstand everyday forces it is subjected to in a physiological environment. The bone substitute consequently must have similar material properties to bone. A mismatch in those material properties can lead to loosening at the bone replacement interface [42]. Volumetric porosity must exist in the bone replacement for bone to incorporate into the bone replacement [23]. A method to create and direct interconnected porosity in epoxy was established in this study. The method used to create interconnected porosity in epoxy also has potential to be used for fiber reinforced epoxy. For long-term considerations, the procedure to create such a bone replacement should be cost effective and time efficient without compromising quality.

Comparison of elastic modulus between thicknesses of each material revealed a statistically significant difference in the 30 wt% ZTA beams. Significant difference for the 30 wt% ZTA beams indicated that the method of manufacturing such ceramic beams was inconsistent. Inconsistency in manufacturing the ceramic beams was also visually confirmed by the uneven thickness and width of the 30 wt% ZTA beams after firing. Uneven ceramic beams display that the zirconia particles were not evenly dispersed within the alumina matrix. Firing an uneven dispersion of zirconia particles in an alumina matrix caused shrinkage in the area of the beams with an accumulation of zirconia particles. Difficulties with inconsistency in manufacturing of ZTA beams were consistent with previous literature [1].

There were a large number of visible micro cracks on the surface of the 30 wt% beams. Appearance of micro cracks suggested that there was too much zirconia within these beams. The 10 wt% ZTA beams did not display visible micro cracks. However, two of the 20 wt% ZTA beams did have visual micro cracks. Those micro cracks were isolated to one section of the beam. An area of isolated micro cracks indicated the beam had an accumulation of zirconia particles in that area.

The 30 wt% ZTA beams did not completely separate at failure. Incomplete separation confirmed that the zirconia particle reinforcement did in fact reduce the advancement of crack propagation.

Material property testing revealed that all of the materials modulus of elasticity was significantly smaller than bone. This result was not consistent with previous literature for the ZTA [35]. Ultimate stress and yield stress were also significantly smaller than expected for a ceramic [35]. ZTA used for this study can not be used as a bone replacement.

Ultimate stress statistical analysis revealed that none of the bone replacement materials used in this study were similar to bone. The ultimate stress statistical analysis results do raise a concern. The materials selected for this study may fail from a stress smaller than the maximum stress sustained by bone. However, the only time bone reaches ultimate stress is when it fractures. Individuals needing bone replacement likely will not exceed ultimate stress of bone unless they are participating in activities that are not recommended by there physician.

Two of the materials selected for this study had statistically similar yield stress to bone. Yield stress of bone is the maximum stress before it yields and ultimately breaks. The 10 vol% CFRE beams had a mean yield stress of 119 MPa and is the best suited material tested in this study for a bone replacement. 119 MPa yield stress value falls within the range of yield stress (50-150 MPa) range used for bone.

The method used to create interconnected porosity for epoxy in this study allows for control of the porous structure shape dissolved out of epoxy. Pore size can be controlled by the size of the PVA granules used to create the PVA construct. Area of porous epoxy also can be limited to the shape of the PVA construct. Shape of the PVA construct can be limited to the container used to merge the granules. Consequently, the method in this study potentially allows for control of pore size and ability to limit the area of porous epoxy.

4.2 Limitations

The material property testing was done on a three point bending fixture. There is a shear force associated with this type of fixture (Figure A.37). This was taken into consideration and testing speed was performed at 0.2mm/sec to minimize the shear rate. Actual modulus of all tested materials may vary slightly from the reported values because of thickness measurements.

The equation for calculating modulus of elasticity used beam thickness as a factor. Only one beam thickness was used. That dimension was measured near the center of the beam. In order to obtain an accurate thickness for the beams, many values must be taken across the entire beam and then averaged.

ZTA was not sintered, but fired to around 2450 ºF. Sintering to over 3000 ºF will change the material properties of ZTA. Though it may be possible to produce a sufficient bending strength from sintering the ceramic, it is a very stiff, brittle material and has little flexibility. The addition of zirconia to a certain volume percentage as a reinforcing particle may reduce crack propagation (Figure A.38), but this ceramic still is not the best material for flexural applications.

The technique used to create the PVA structure may not be the most efficient polymer merging method. The technique was used simply as a proof of concept. The weight

placed on the PVA granules to increase the contact. The weight is not necessary and is dependant on the researchers desired end result.

A disc shaped PVA structure was used to dissolve out of epoxy to create interconnected porosity. The shape was representative of the container used for the polymer merging technique. The PVA granules can also be changed to any desired size and shape. PVA rods and granules of proper sizes would be a better choice to mimic bones interconnected pores. Trabecular bone pore sizes range from $50 - 450$ μm. Rods of the appropriate size can be used to mimic the interconnecting channels of about 50 μm in diameter [28].

4.3 Future research

The 10 vol% fiber reinforcement was the maximum amount used in the beams. If the amount of fiber content were to be increased, the ultimate stress values will also increase. However, if too much fiber reinforcement is used the mechanical properties of the composite will decrease. The specific epoxy resin system used was difficult to handle with over 10 vol% carbon fiber reinforcement (CFR). Difficulty handling suggests good carbon fiber matrix adhesion. The adhesion between the fiber and matrix is very important because this is how the load is effectively transferred to the fibers [48]. Future research needs to be done to determine the optimal volume percent of fiber reinforcement in the proper epoxy resin system.

It is unknown how effective the method used to create porosity can be for fiber reinforced epoxy. Initial testing indicates the method to create an interconnected porous structure in carbon and glass fiber reinforced epoxy to have potential. If the method to create porosity is effective, it must be determined what effect it has on the fiber bonding to epoxy. The mild phosphoric acid may alter the surface of the fibers. The fibers trapped between PVA also may not be coated by the epoxy poured over the structure. An insufficient amount of fiber coated by epoxy can affect the material properties that the reinforcing fibers were intended for.

Future testing can include compression tests on the porous fiber reinforced epoxy (FRE) structure. Simple beams can also be manufactured and tested after wetting the fibers with mild phosphoric acid. Those beams can then be subjected to the same material property tests as beams with fibers not wetted with mild phosphoric acid. A test to see whether the glass transition temperature of the polymer is altered after the use of mild phosphoric acid should also be done.

Selection of the correct polymer to dissolution out of epoxy requires an understanding of the material and application in which it is being used. The slight affinity towards water, observed during the wetting test of the epoxy resin led me to believe that the polymer material should not be readily dissolvable in water. Polymers not readily dissolvable in water led to the reasoning that PVA may be a good material selection for this application. PVA must be raised to a certain temperature in order to readily dissolve in water. The 125,000 molecular weight and 88% hydrolysis PVA worked for this study. However, it is unknown which PVA molecular weight and percent hydrolysis is best suited for this application. The best suited PVA for this application can be determined by imbedding the PVA granules in epoxy followed by dissolution of PVA granules in water. The best suited PVA for this application will dissolution in the shortest amount of time.

Appendices

What membrane lines the internal canals and covers the trabeculae of spongy bone?

Lamella

Osteocyte

Osteon (Haversian system)

Circumferential lamellae

Lamellae

Lacuna

Canaliculus

Central (Haversian) canal

Blood vessel continues into medullary cavity containing marrow

Spongy bone

Osteon

Sharpey's fibers

Compact bone

Periosteal blood vessel

Periosteum

Central (Haversian) canal

Perforating (Volkmann's) canal

Blood vessel

(a)

(b)

Human Anatomy and Physiology 4th Ed., Elaine N.Marieb

Figure A.1 - Long bone macroscopic and microscopic structure.

Appendix A (Continued)
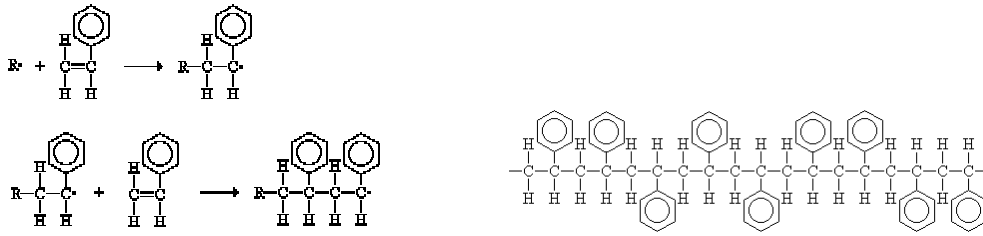
Figure A.2 – Polymerization chain-reaction initiated by a free radical.

A chemical reaction that links monomers into a polymer chain.
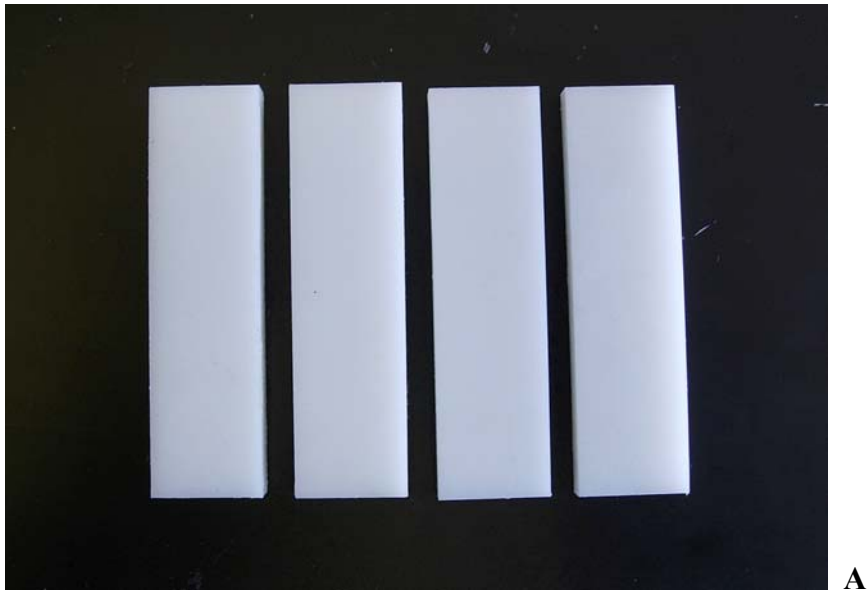
A
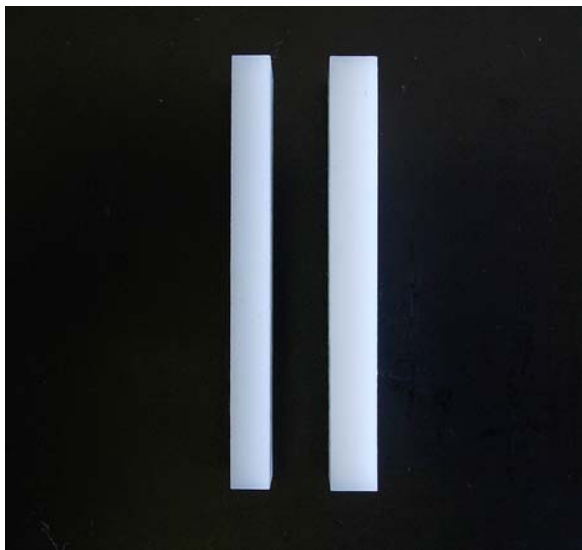
B

Figure A.3 – Plastic beams used for silicone rubber mold

A**:** Frontal view of plastic beams

B**:** Side view of plastic beams

Figure A.4 – Box fabricated for pouring the silicone rubber molding. The box was held together by epoxy.
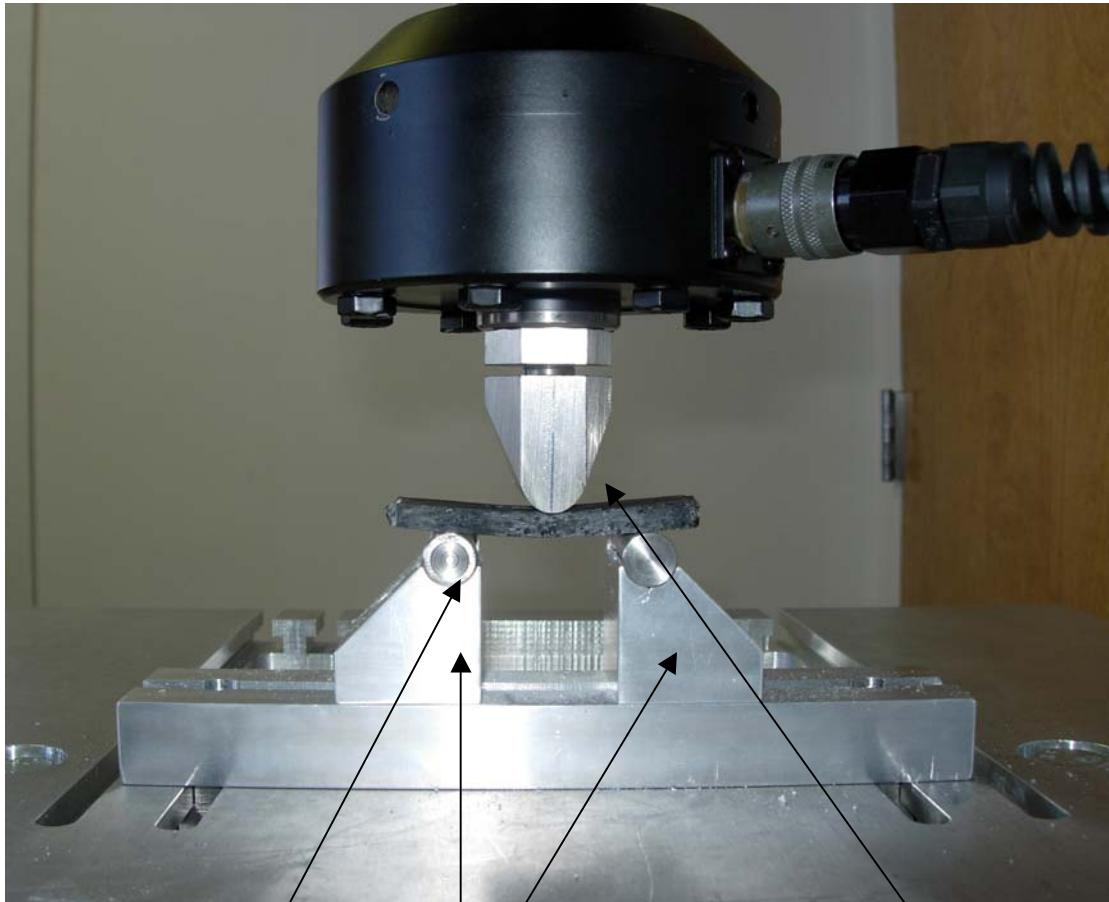
Roller   Adjustable supports   Bending post

Figure A.5- Three point bending fixture with CFRE beam specimen being tested.

Appendix A (Continued)
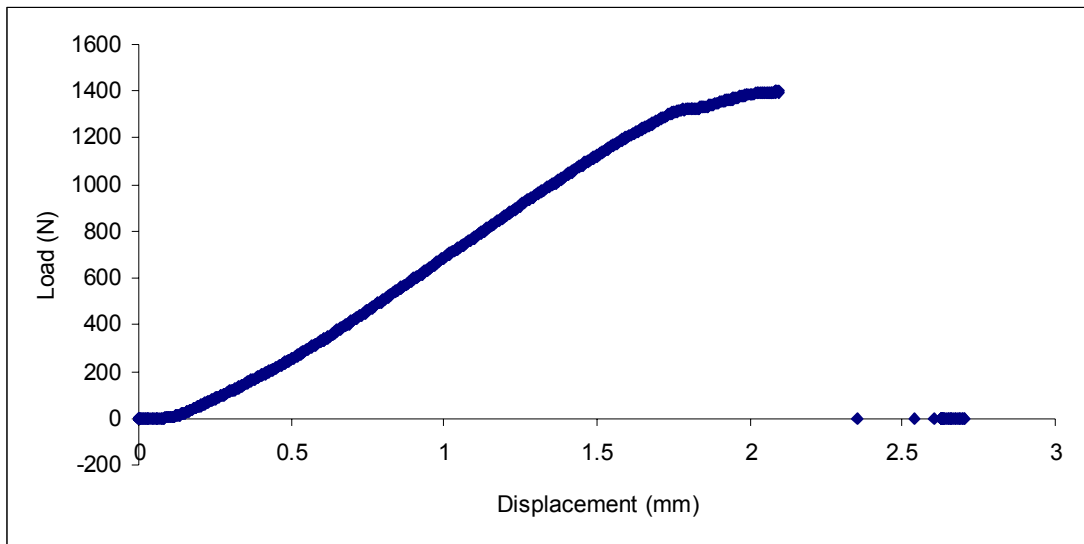
Figure A.6 - Example load-displacement curve from collected data for beams in three-point bending.

Appendix A (Continued)
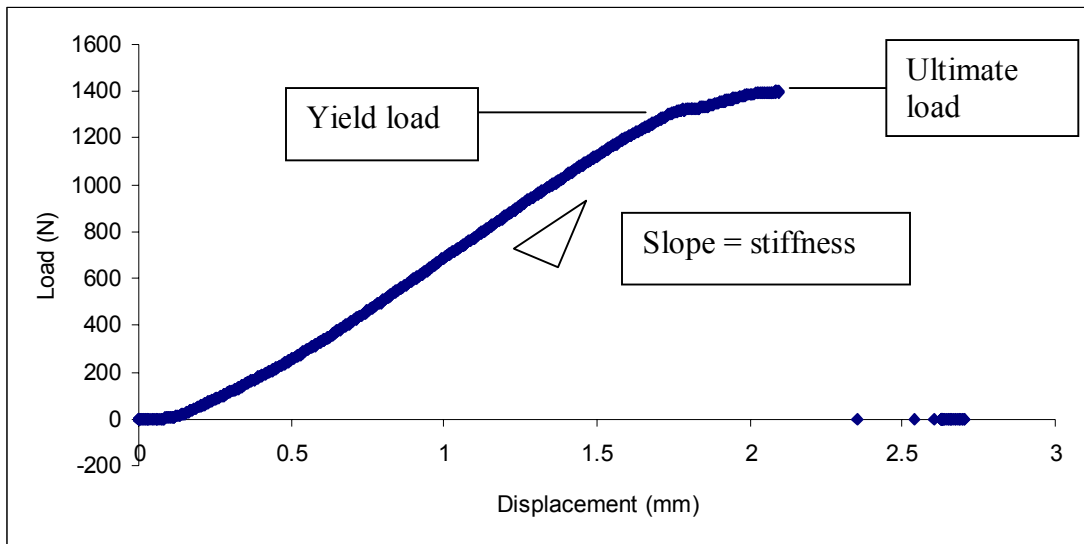
Figure A.7 - Location of values on load versus displacement curves used to calculate material properties.

Appendix A (Continued)
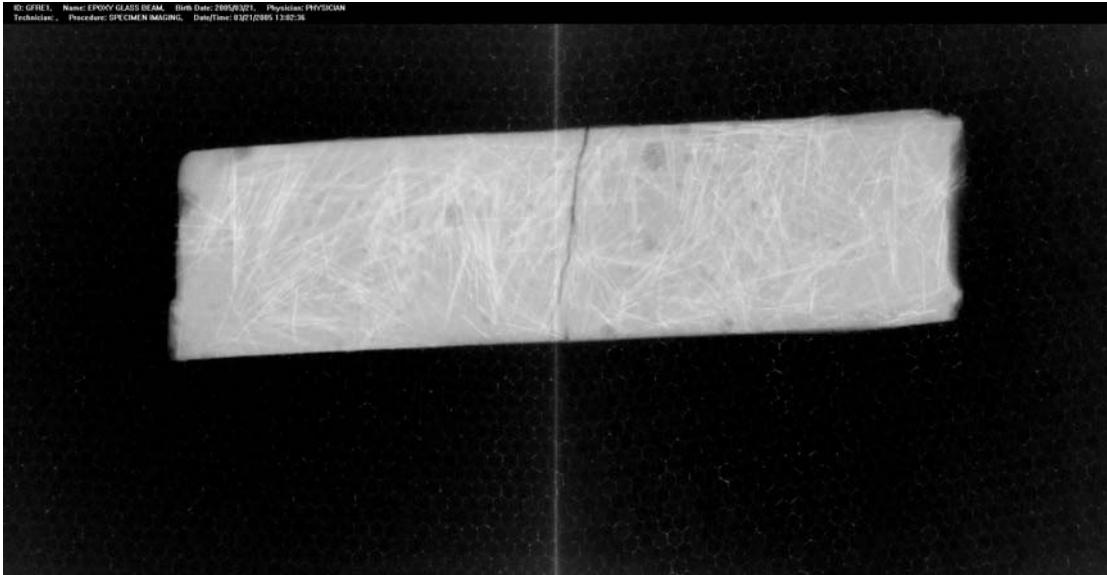
Figure A.8 – One vol% GFRE beam X-ray image used to estimate fiber orientation.
Fiber orientation in the 1 vol% GFRE beams was largest in the range of 70-110 degrees
from the horizontal axis.

Figure A.9 - Ten vol% GFRE beam X-ray image used to estimate fiber orientation. Fiber orientation of the 10 vol% GFRE was largest in the length wise direction of the beams.

Appendix A (Continued)

```
┌─────────────────────────────────────┐
│  Place PVA granules in desired container │
│                shape                     │
└─────────────────────────────────────┘
                    │
┌─────────────────────────────────────┐
│  Wet PVA granules with dilute phosphoric │
│                acid                      │
└─────────────────────────────────────┘
                    │
┌─────────────────────────────────────┐
│ Place weight on barrier over PVA granules for a few │
│    minutes and allow them to merge overnight        │
└─────────────────────────────────────┘
                    │
┌─────────────────────────────────────┐
│  Remove merged PVA from container after │
│  24 hours or until it has completely dried │
│              (Figure 4A)                 │
└─────────────────────────────────────┘
                    │
┌─────────────────────────────────────┐
│   Pour mixed epoxy material over PVA     │
│              structure                   │
└─────────────────────────────────────┘
                    │
┌─────────────────────────────────────┐
│ Remove PVA/epoxy block from container after │
│           curing (Figure 4B)             │
└─────────────────────────────────────┘
                    │
┌─────────────────────────────────────┐
│  Remove surface of PVA/Epoxy to expose PVA │
│              (Figure 4C)                 │
└─────────────────────────────────────┘
                    │
┌─────────────────────────────────────┐
│ Place material in warm water to dissolve out the │
│              PVA structure               │
└─────────────────────────────────────┘
```

Figure A.10 – Process flow chart for method to create interconnected porosity in epoxy.
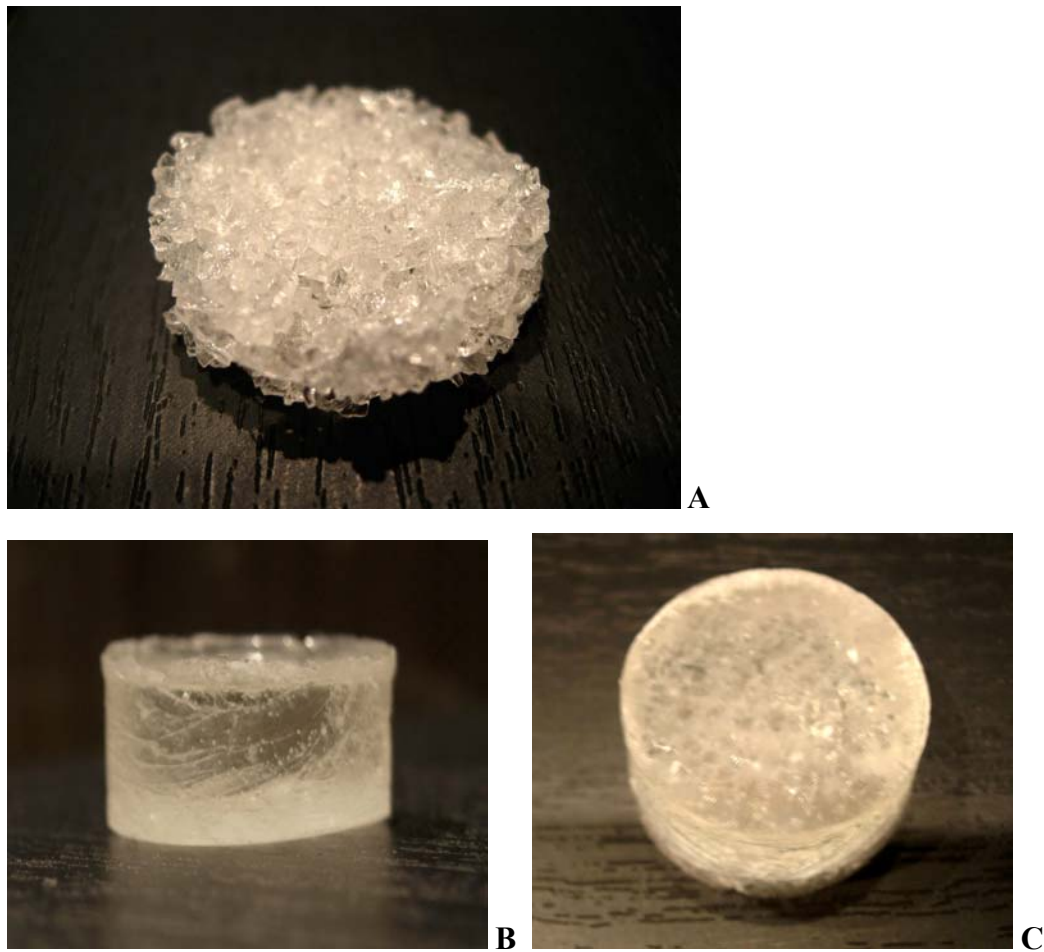
Figure A.11 - Epoxy/PVA construct

A: Porous construct of merged PVA granules.

B: Formed epoxy disc with embedded PVA construct.

C: Exposed PVA granules after surface removal.

Appendix A (Continued)
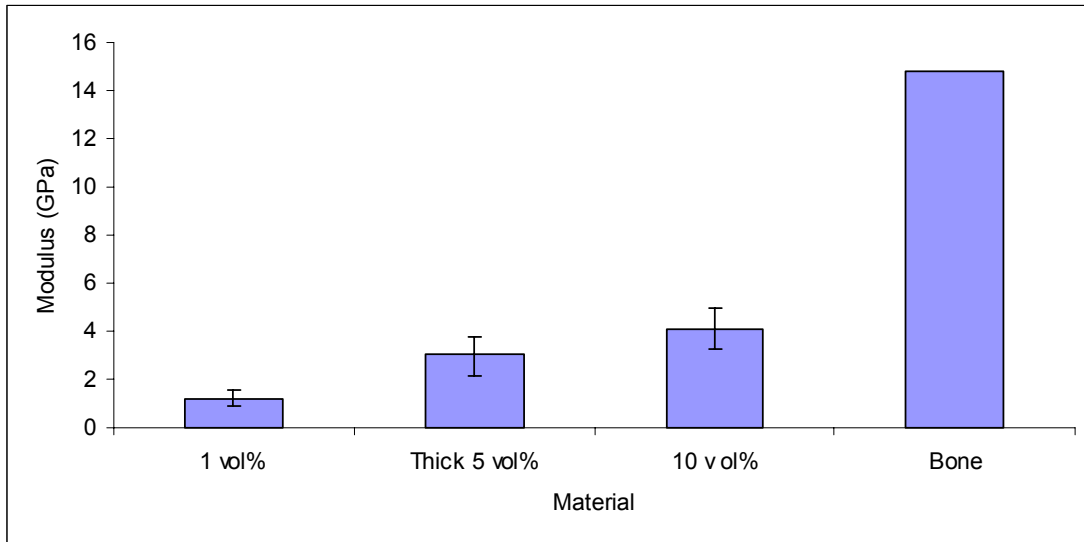
Figure A.12 - Modulus comparison between bone and different volume percentage CFRE beams. Means and ranges are reported for the different CFRE groups.
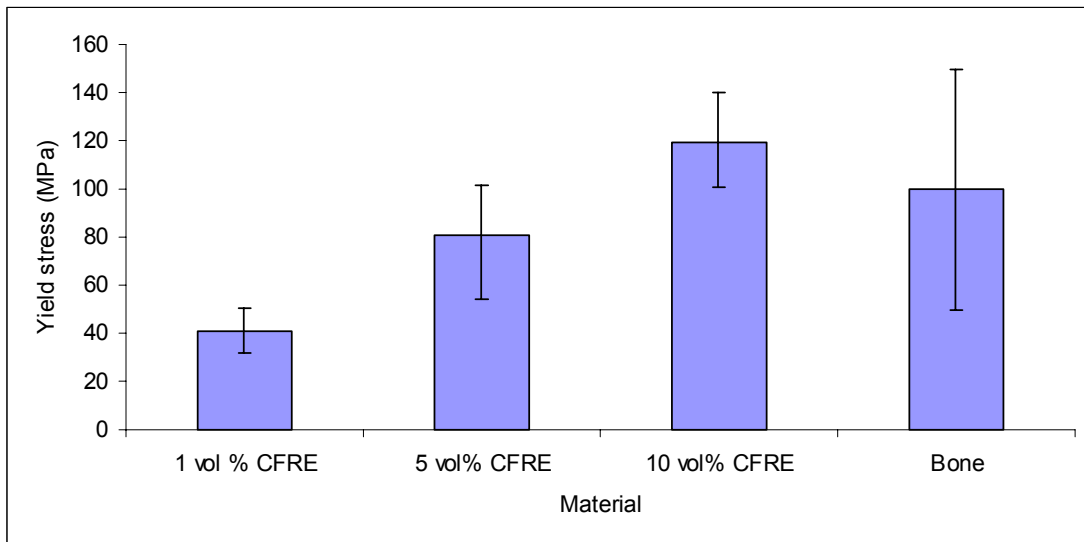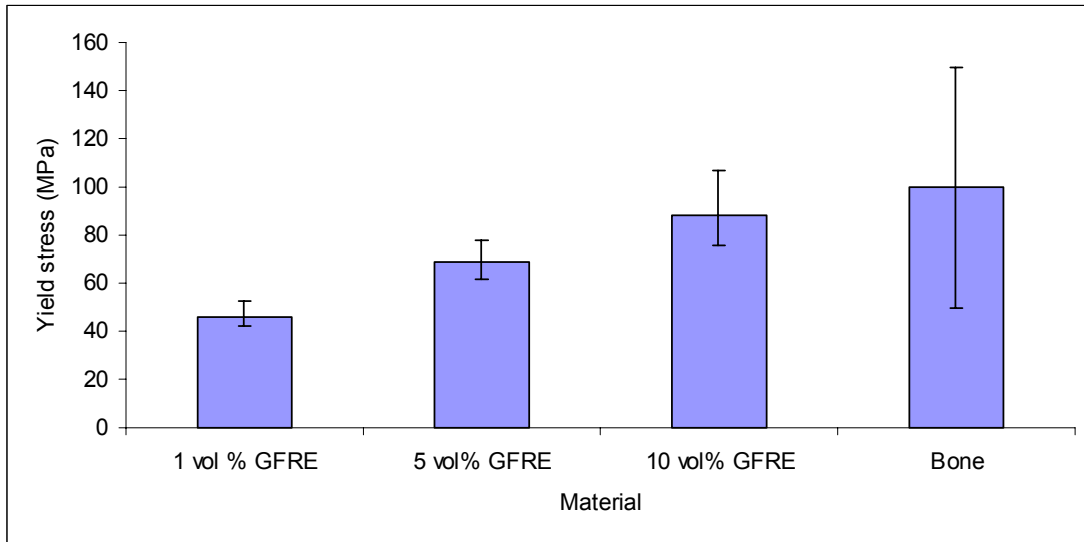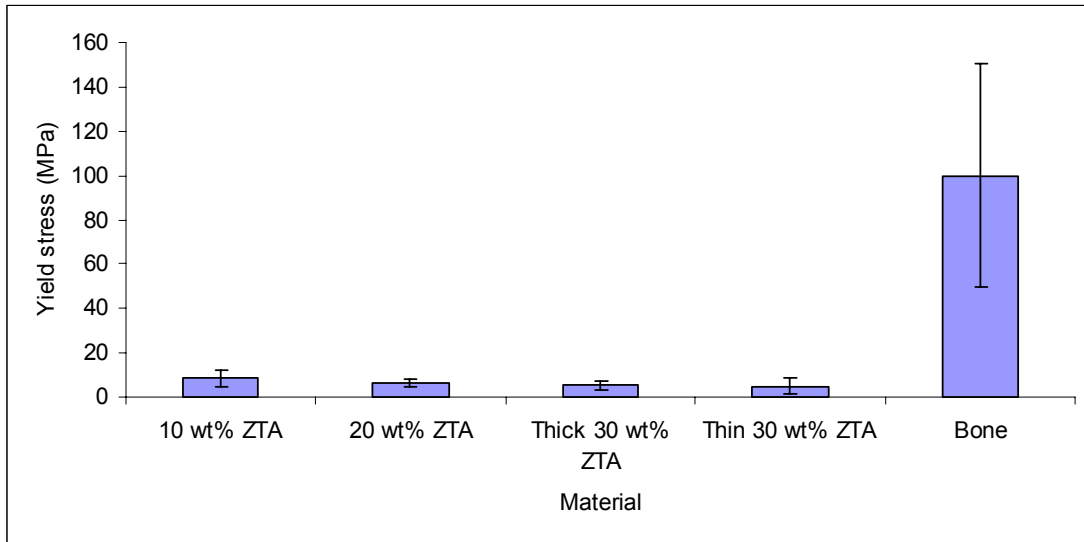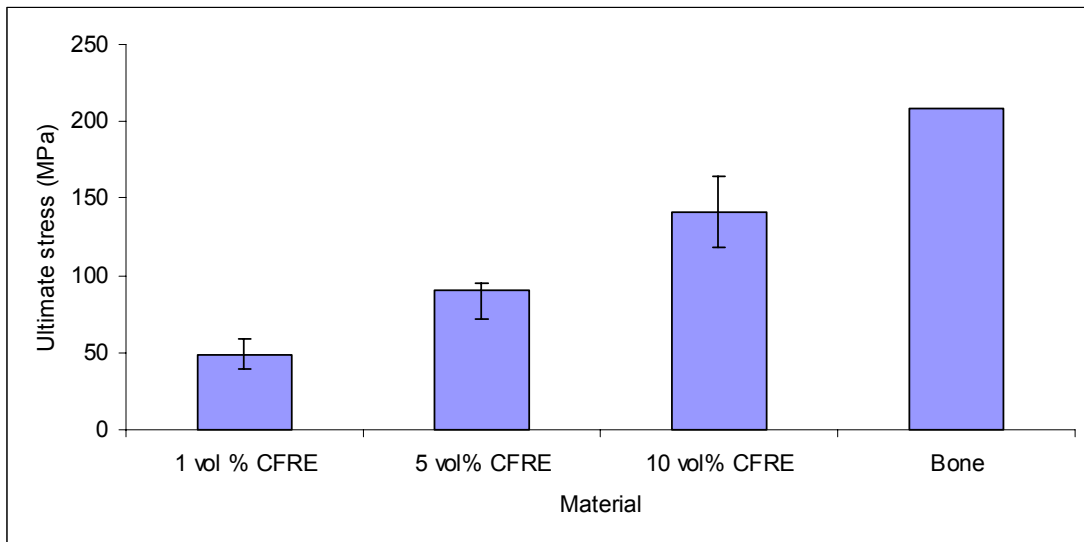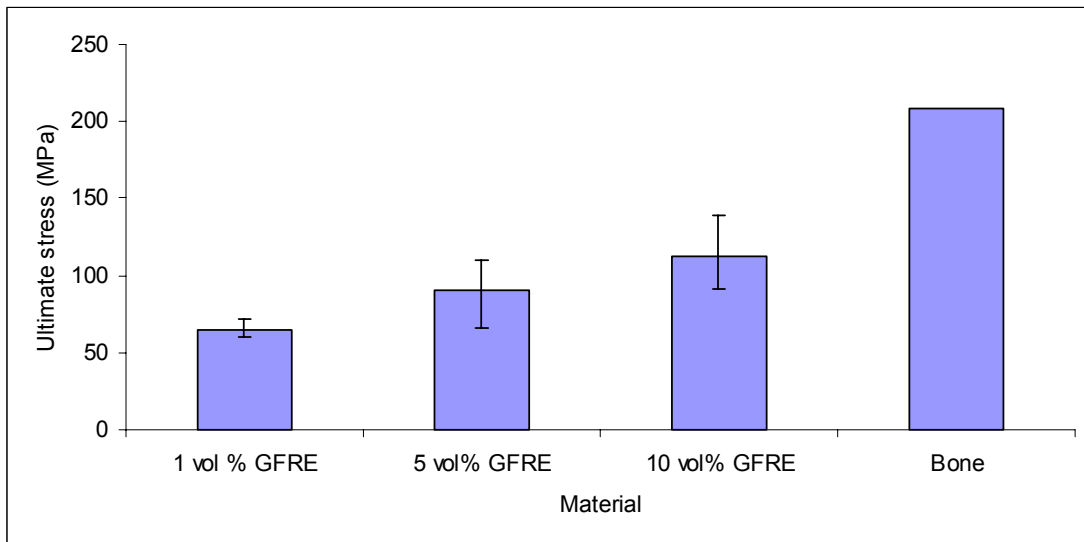
Appendix A (Continued)
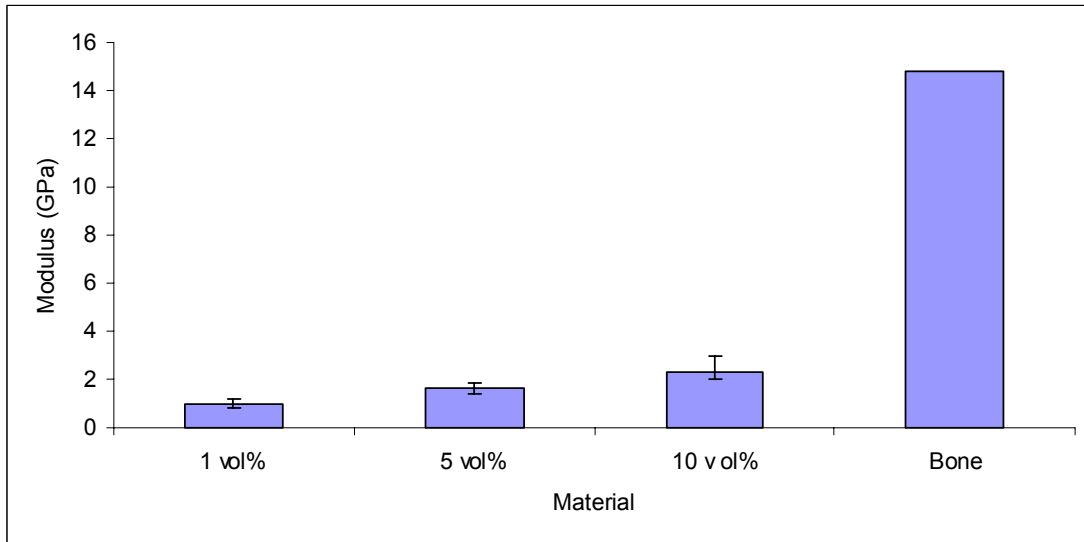
Figure A.13 - Modulus comparison between bone and different volume percentage GFRE beams. Means and ranges are reported for the different GFRE groups.
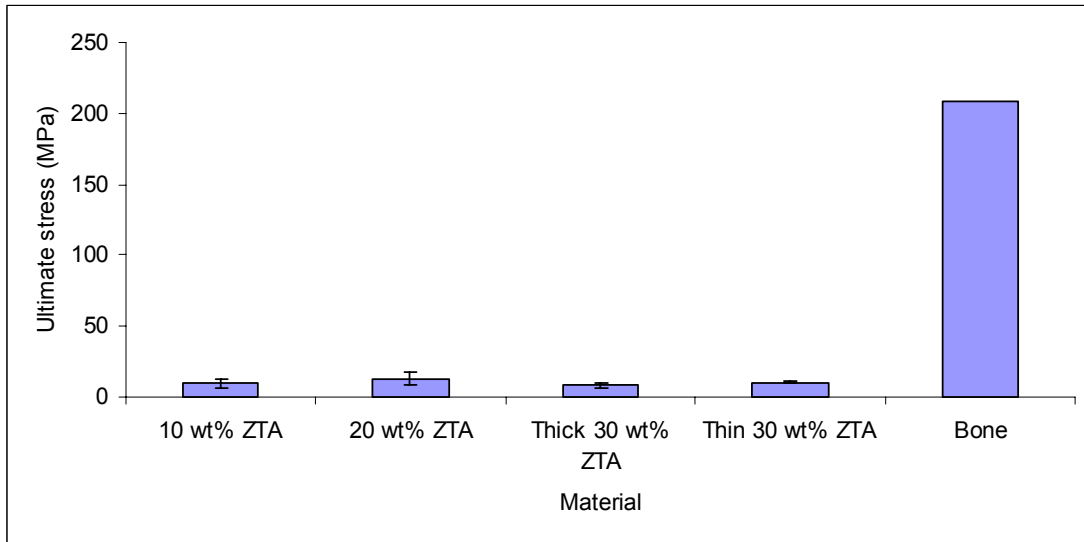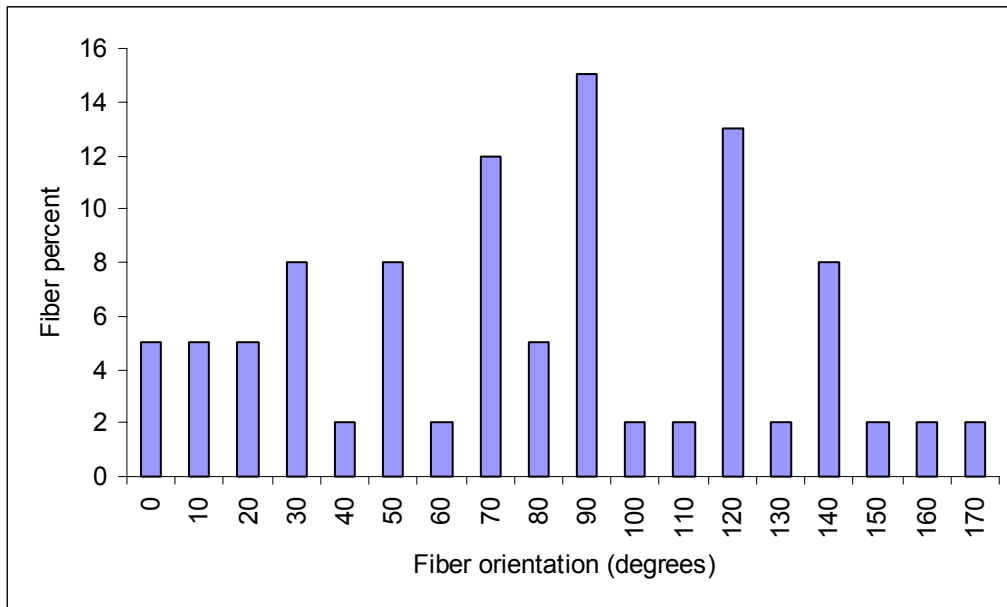
Appendix A (Continued)
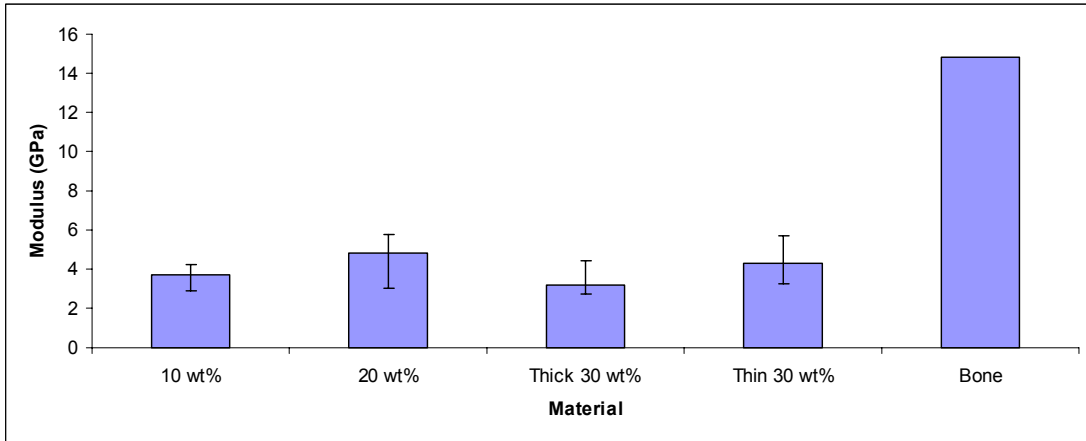
Figure A.14 - Modulus comparison between bone and different volume percentage ZTA beams. Means and ranges are reported for the different GFRE groups.

Figure A.15 - Yield stress comparison between bone and different volume percentage CFRE beams. Means and ranges are reported for the all groups. The 10 vol% CFRE beams was the highest mean yield strength for all materials.

Figure A.16 - Yield stress comparison between bone and different volume percentage GFRE beams. Means and ranges are reported for the all groups.

Figure A.17 - Yield stress comparison between bone and different volume percentage ZTA beams. Means and ranges are reported for the all groups.

Figure A.18 - Ultimate stress comparison between bone and different volume percentage CFRE beams. The 10 vol% CFRE beams was the highest mean ultimate strength for all materials compared to bone. Means and ranges are reported for the different CFRE groups.

Appendix A (Continued)

Figure A.19 - Ultimate stress comparison between bone and different volume percentage GFRE beams. Means and ranges are reported for the different GFRE groups.

Appendix A (Continued)

Figure A.20 - Ultimate stress comparison between bone and different volume percentage ZTA beams. Means and ranges are reported for the different ZTA groups.

Figure A.21 - Approximate fiber orientation of one volume percent glass fiber reinforced epoxy (specimen #1). Note: Fiber percent values are in generic units.
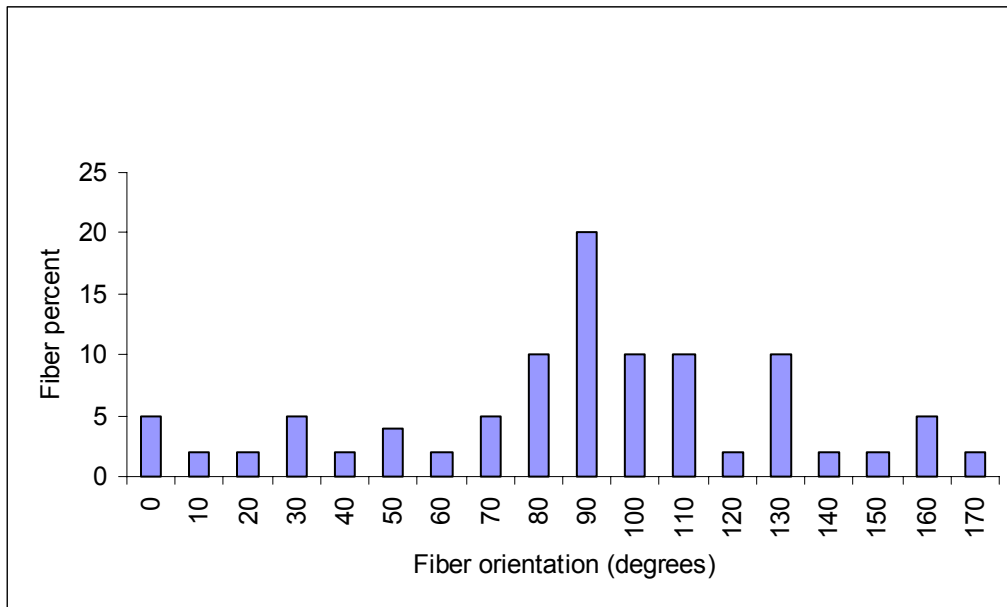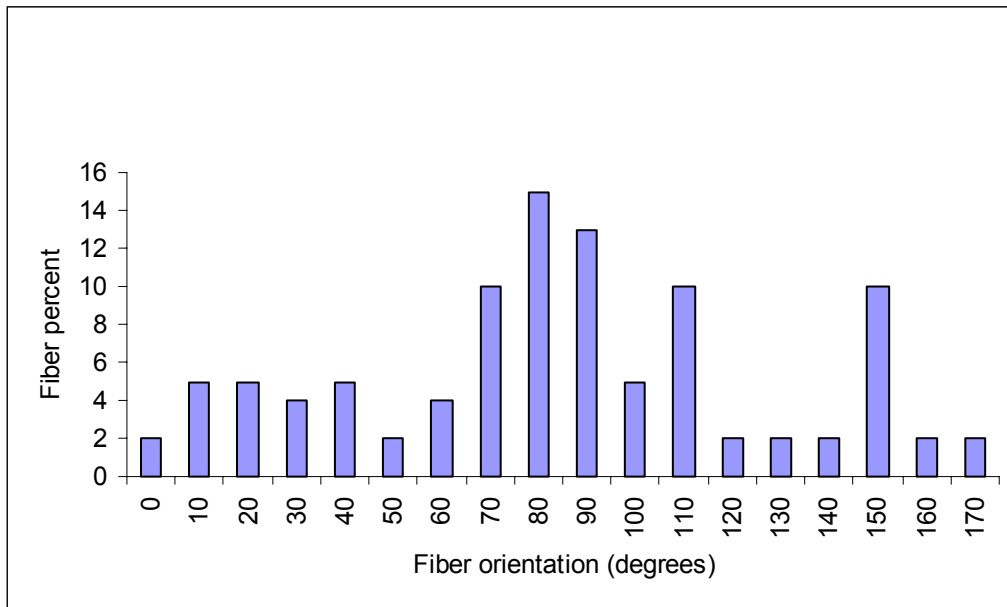
Appendix A (Continued)
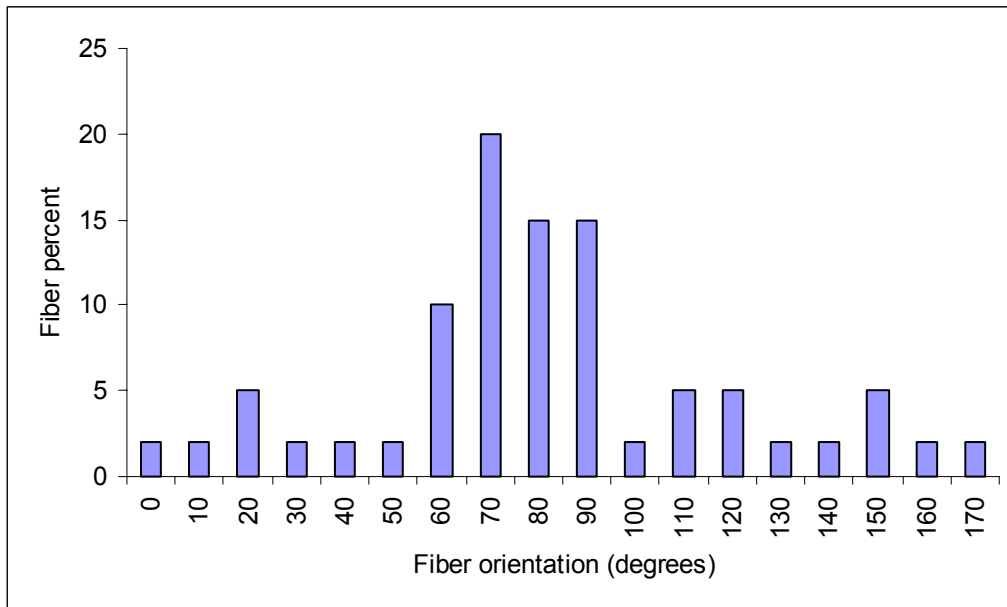
Figure A.22 - Approximate fiber orientation of one volume percent glass fiber reinforced epoxy (specimen #2). Note: Fiber percent values are in generic units.
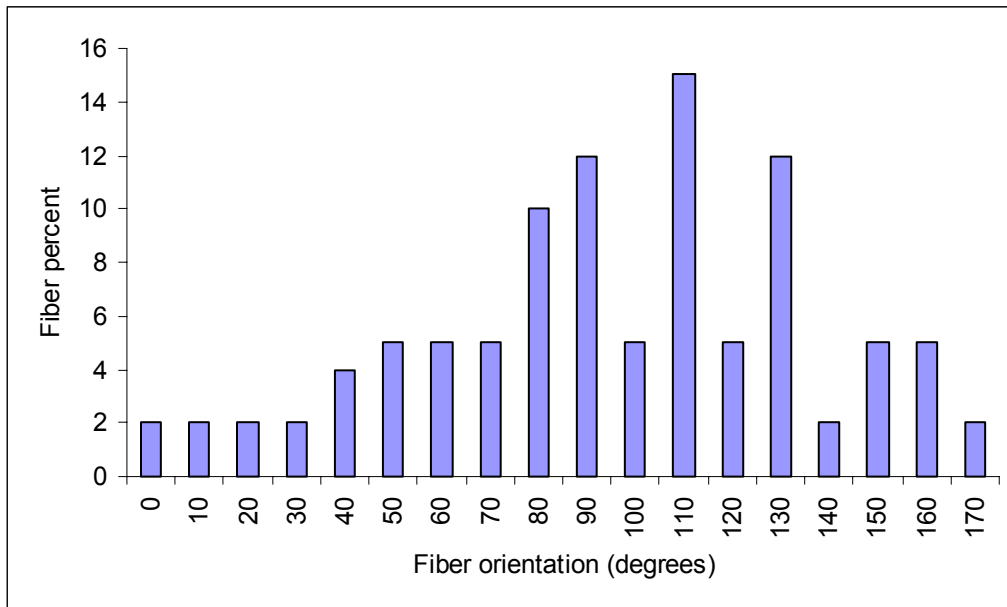
Figure A.23 - Approximate fiber orientation of one volume percent glass fiber reinforced epoxy (specimen #3). Note: Fiber percent values are in generic units.
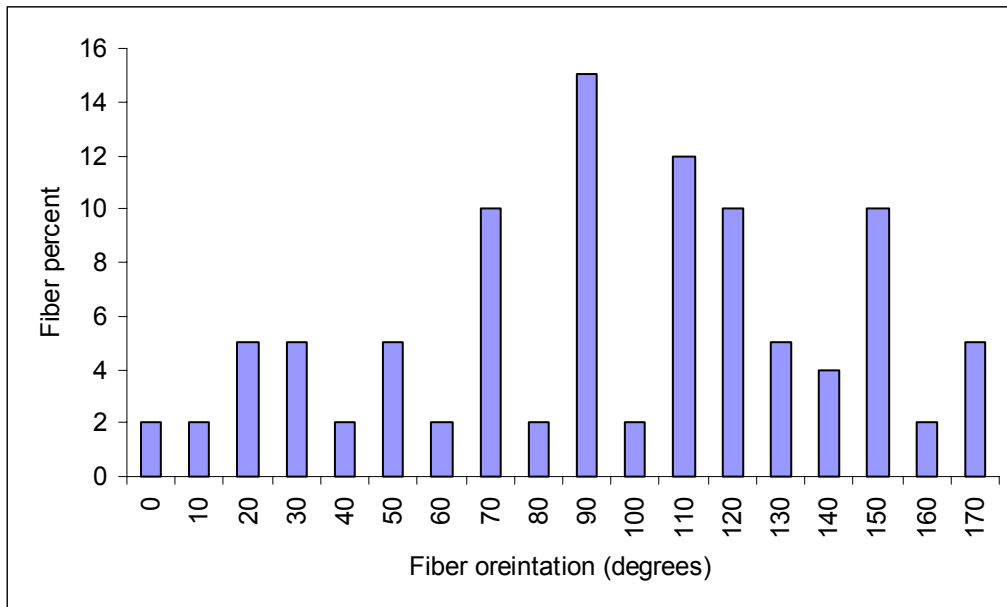
Figure A.24 - Approximate fiber orientation of one volume percent glass fiber reinforced epoxy (specimen #4). Note: Fiber percent values are in generic units.
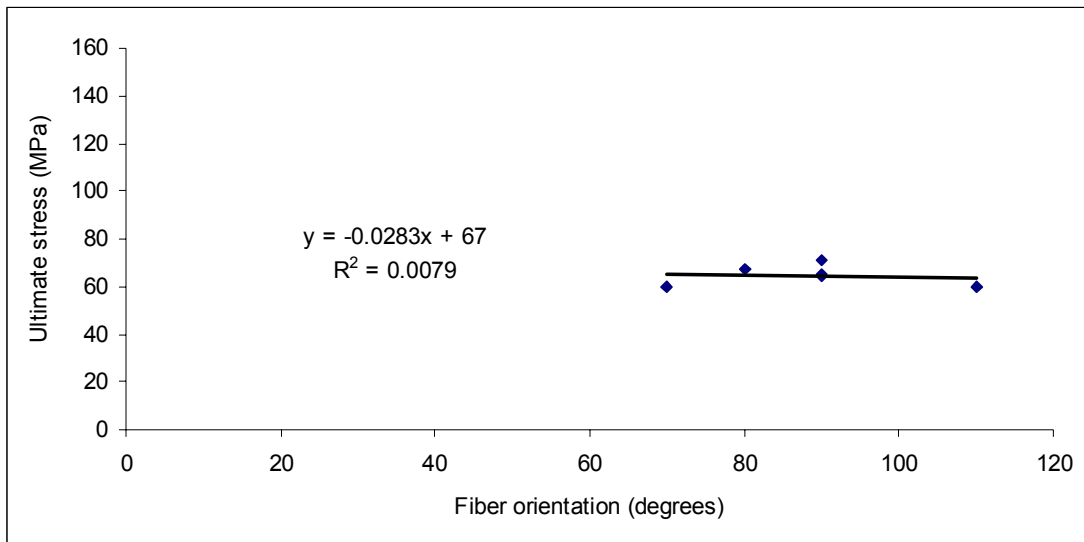
Appendix A (Continued)

Figure A.25 - Approximate fiber orientation of one volume percent glass fiber reinforced epoxy (specimen #5). Note: Fiber percent values are in generic units.

Appendix A (Continued)

Figure A.26 **-** Approximate fiber orientation of one volume percent glass fiber reinforced epoxy (specimen #6). Note: Fiber percent values are in generic units.

Figure A.27 - Correlation between fiber orientation and ultimate stress in 1 vol% GFRE beams. There was no correlation between fiber orientation and ultimate stress for the 1 vol% GFRE.
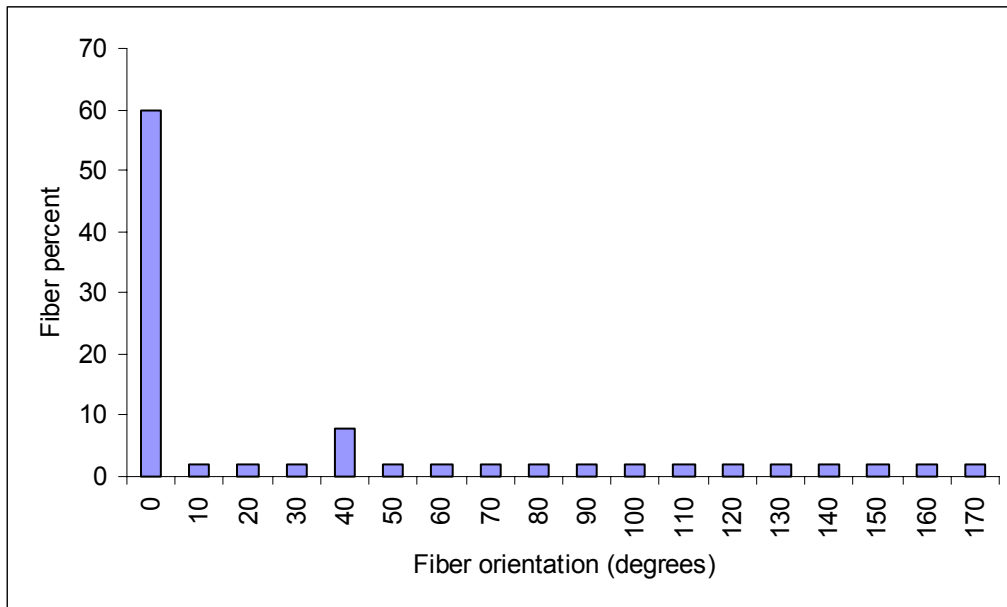
Appendix A (Continued)

Figure A.28- Approximate fiber orientation of ten volume percent glass fiber reinforced epoxy (specimen #1). Note: Fiber percent values are in generic units.
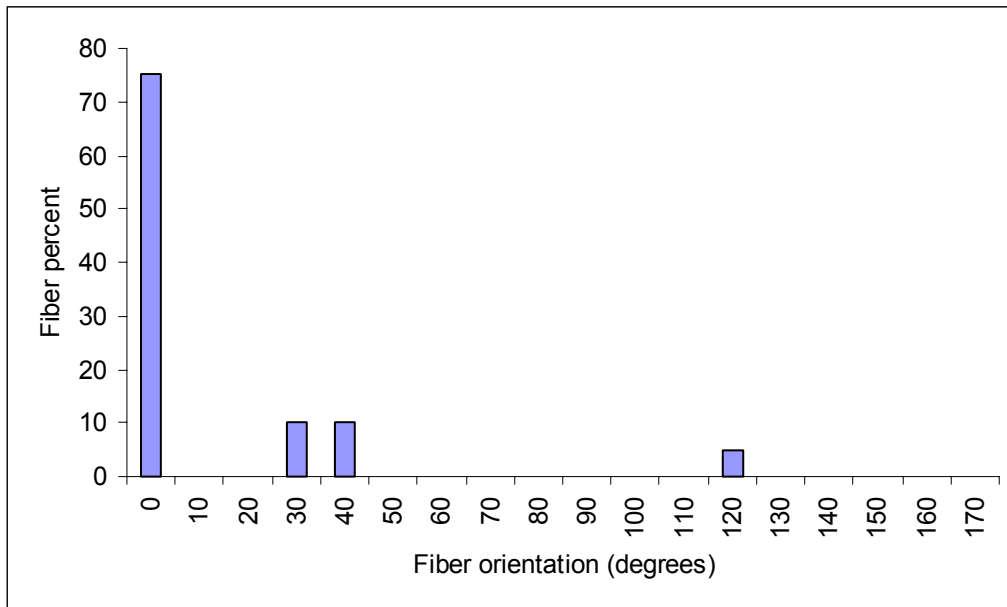
Figure A.29 - Approximate fiber orientation of ten volume percent glass fiber reinforced epoxy (specimen #2). Note: Fiber percent values are in generic units.
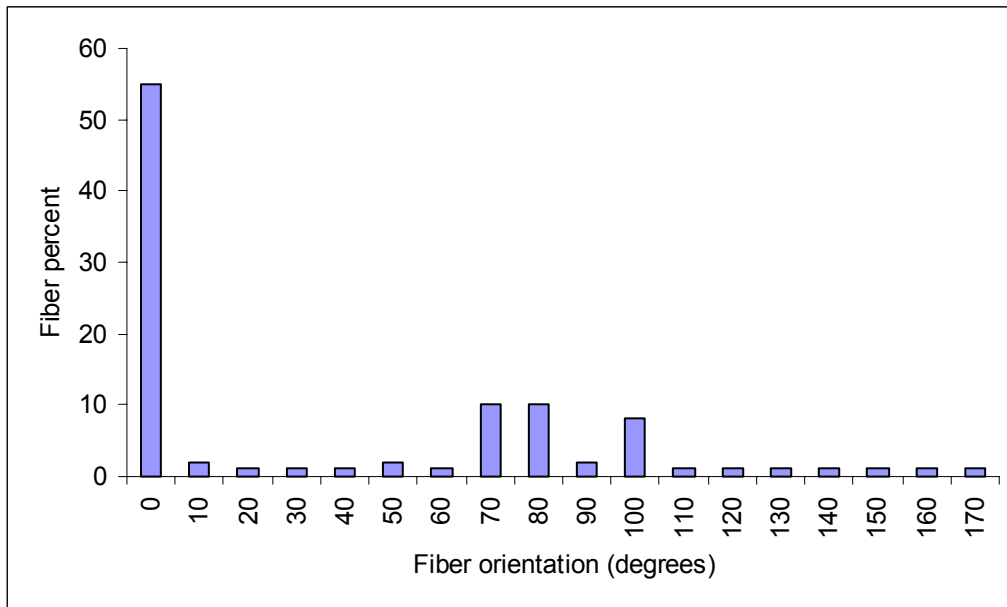
Appendix A (Continued)

Figure A.30 - Approximate fiber orientation of ten volume percent glass fiber reinforced epoxy (specimen #3). Note: Fiber percent values are in generic units.
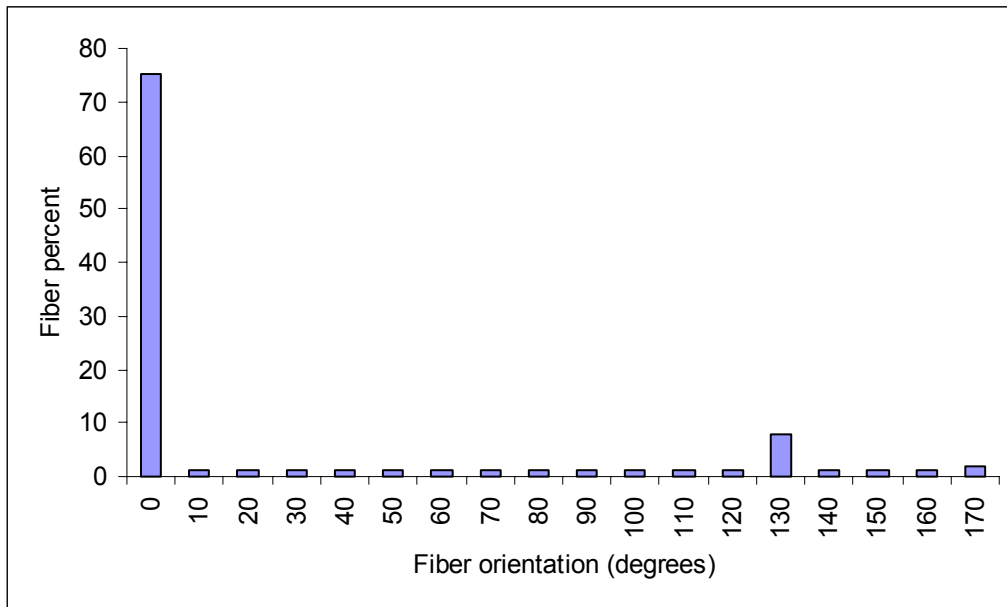
Figure A.31 - Approximate fiber orientation of ten volume percent glass fiber reinforced epoxy (specimen #4). Note: Fiber percent values are in generic units.

Figure A.32 **-** Approximate fiber orientation of ten volume percent glass fiber reinforced epoxy (specimen #5). Note: Fiber percent values are in generic units.

Appendix A (Continued)

Figure A.33 - Approximate fiber orientation of ten volume percent glass fiber reinforced epoxy (specimen #6). Note: Fiber percent values are in generic units.

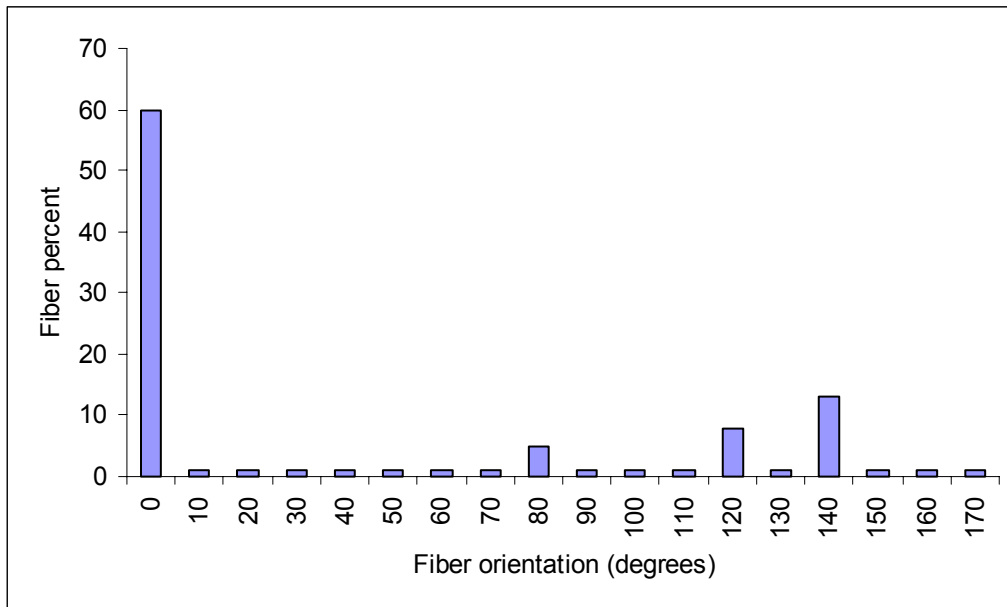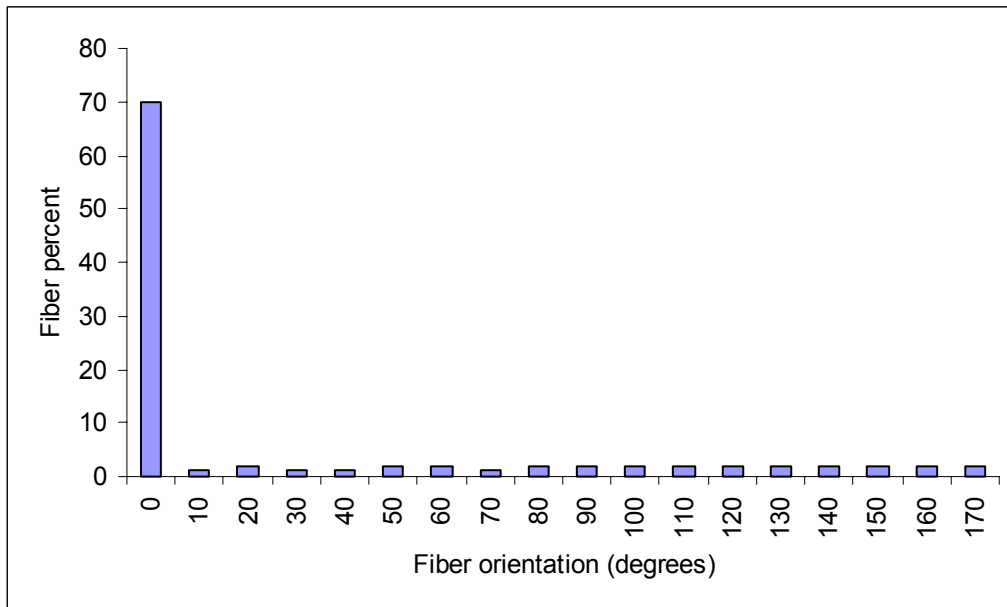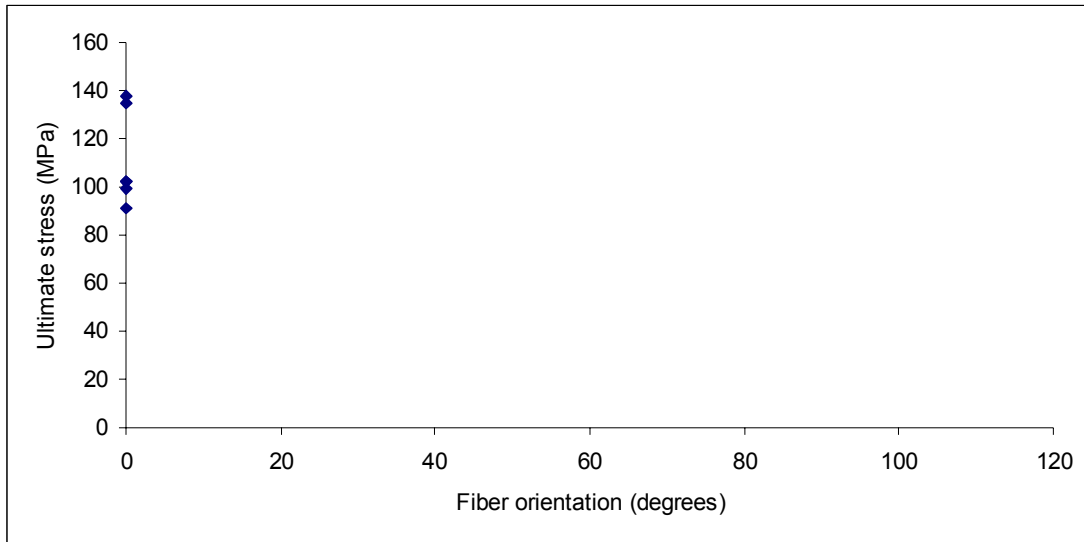Appendix A (Continued)

Figure A.34 - Correlation graph for fiber orientation to ultimate stress in 10 vol% GFRE beams. There was no correlation between fiber orientation and ultimate stress for the 10 vol% GFRE.
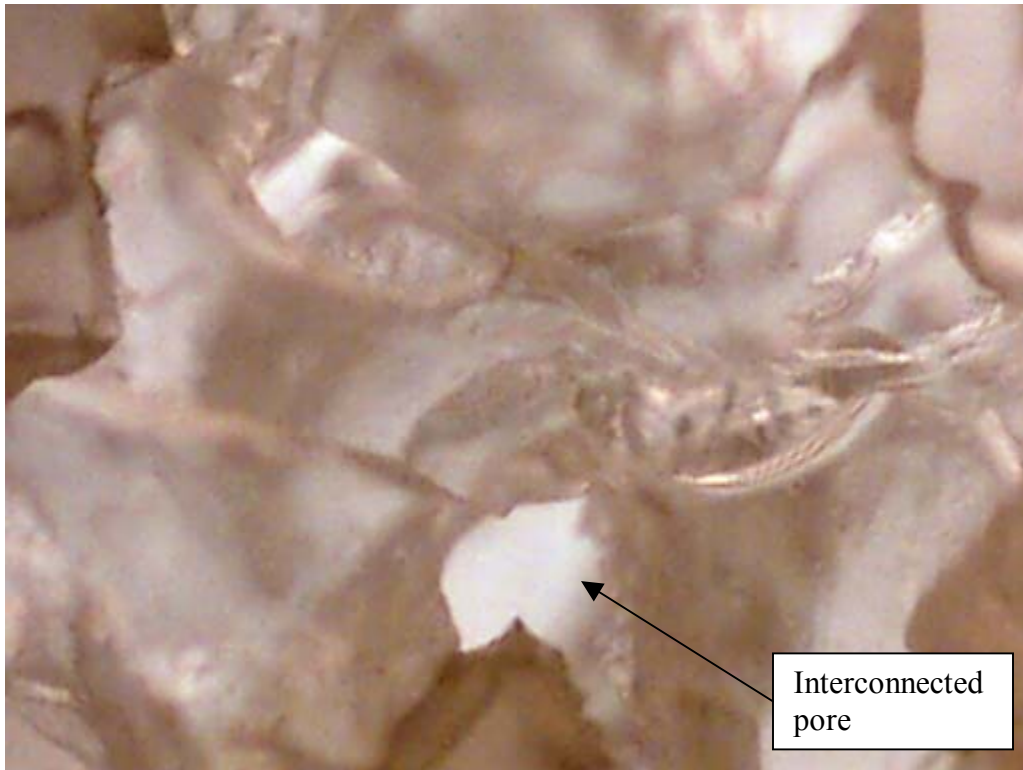
Figure A.35 **-** Interconnected porous epoxy disc, 60x magnification.
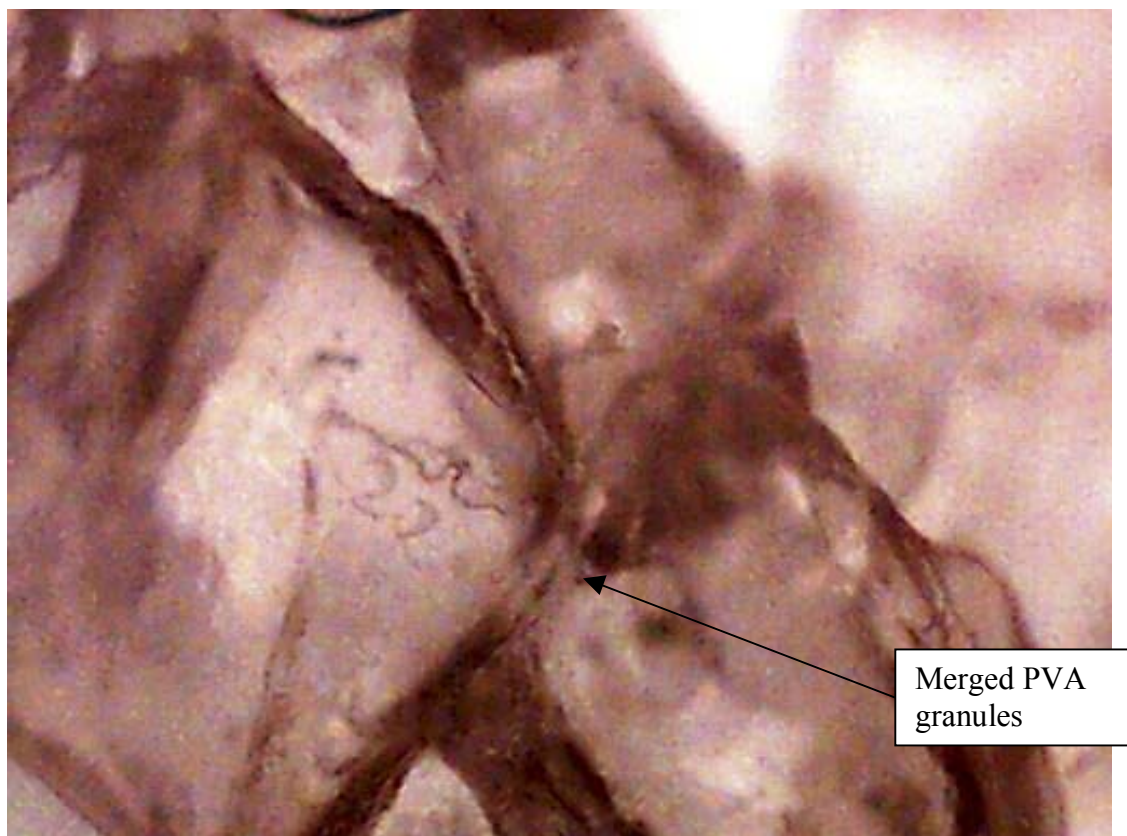
Figure A.36 – Merged PVA granules dissolved out of epoxy disc, 60x magnification.
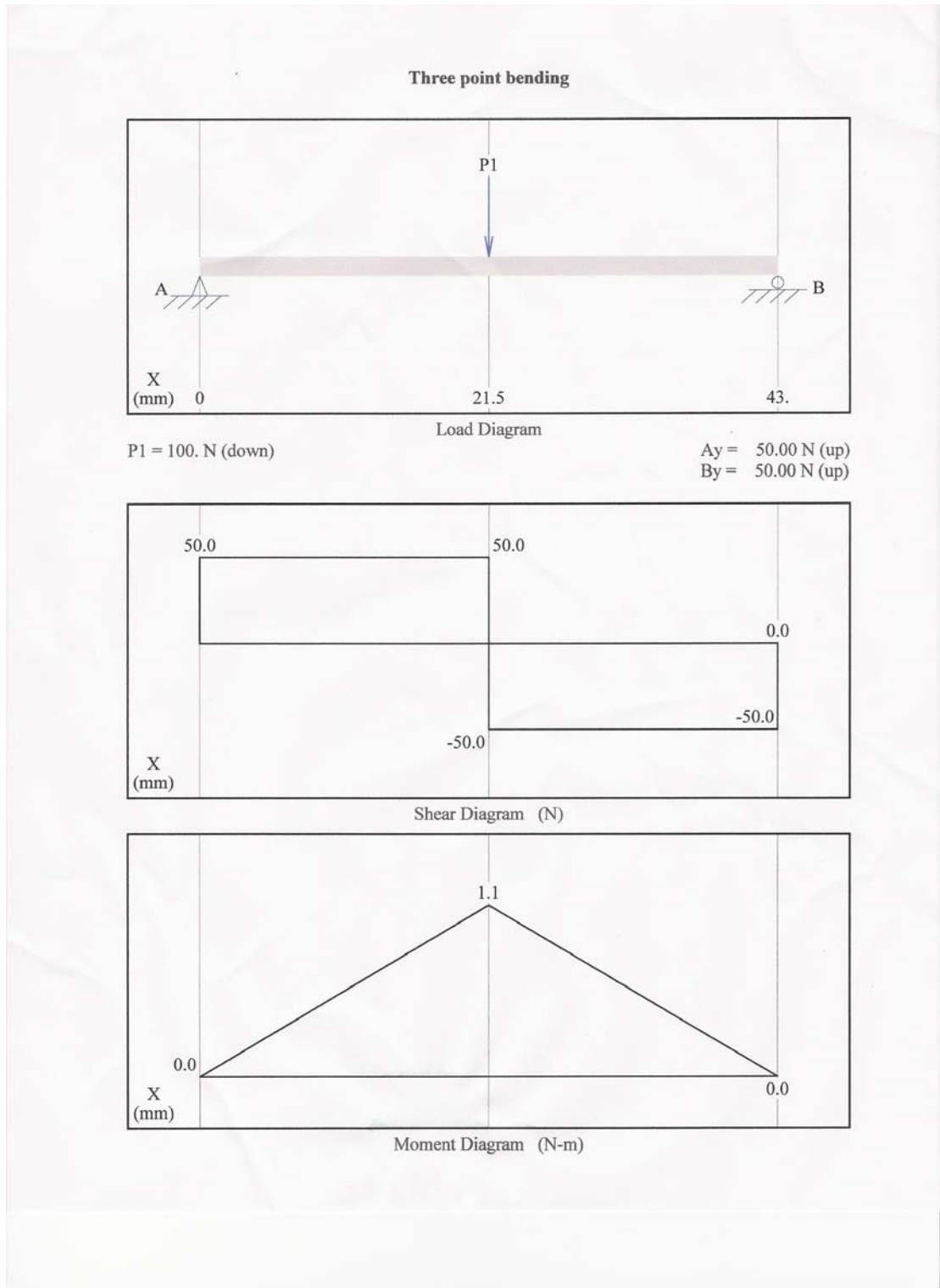
Appendix A (Continued)

Figure from MD Solids software

Figure A.37 - Three point bending load diagram, shear diagram, and moment diagram.
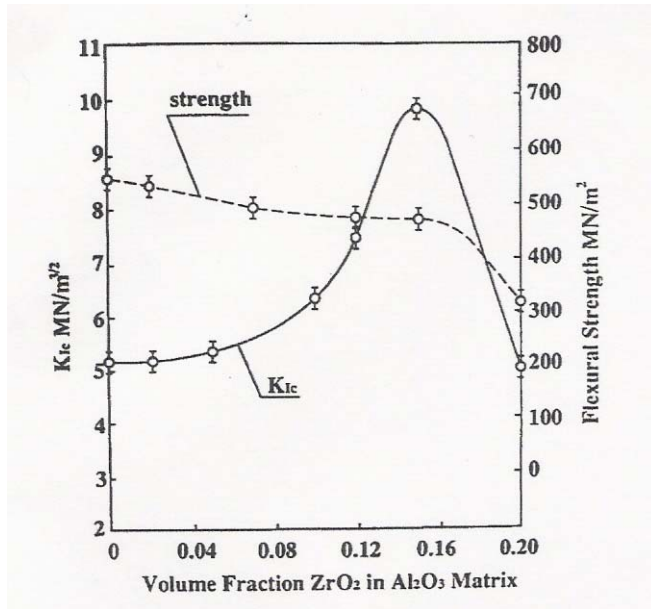
Appendix A (Continued)

Figure A.38 – Fracture toughness and flexural strength for ZTA of different volume fractions of zirconia in alumina.

Appendix B – Tables

Beam material	Mean stiffness (N/mm)	Mean yield force (N)	Mean ultimate force (N)
Thick 1 vol% CFRE	276.11	443.33	530.17
Thick 5 vol% CFRE	754.34	947.5	1059.5
Thick 10 vol% CFRE	979.74	1360	1618.33
Thin 1 vol% CFRE	187.74	340.17	437.67
Thin 5 vol% CFRE	377.40	533.33	615
Thin 10 vol% CFRE	615.18	896.67	1031.5
Thick 1 vol% GFRE	246.24	555	791.5
Thick 5 vol% GFRE	463.63	875.83	1147
Thick 10 vol% GFRE	616.50	1095.83	1390.5
Thin 1 vol% GFRE	127.82	315.17	431.83
Thin 5 vol% GFRE	278.32	618.33	736
Thin 10 vol% GFRE	399.23	829.5	980.33
Thick 10 wt% ZTA	933.02	106.67	128.83
Thick 20 wt% ZTA	1098.56	66	136.5
Thick 30 wt% ZTA	517.14	44	70.67
Thin 10 wt% ZTA	399.23	62	88
Thin 20 wt% ZTA	620.81	56.33	82.66
Thin 30 wt% ZTA	438.28	31.5	60.67

Table B.1 **-** Load-displacement curve values to calculate material property values.

Appendix B (Continued)

Line 1	3.54 + 0.39 + 0.33 + 0.21 = 4.47 mm
Line 2	2.3 + 1.47 + 1.0 + 0.7 + 0.6 + 0.72 = 6.79 mm
Line 3	3.1 + 0.91 + 0.78 + 2.55 = 7.34 mm
Line 4	1.6 + 2.43 + 0.54 + 0.89 + 0.68 = 6.14 mm
Line 5	3.26 + 0.92 + 1.1 + 0.7 + 1.15 = 7.13mm
Line 6	2.85 + 0.83 + 0.75 + 1.2 + 0.95 = 6.58 mm
Total	[(4.47 + 6.79 + 7.34 + 6.14 + 7.13 + 6.58)/ 6x13] x 100 = 49.3%

Table B.2 **-** Stereology test results for approximate void area in epoxy disc. Note: Total value is given in generic units.

References

1. Agarwal DC: "Advanced Ceramics." Technology: Advanced Ceramics, 3, 4, July 2000.

2. Almirall A, Larrecq G, Delgado JA, Martinez S, Planell JA, Ginebra MP: "Fabrication of low temperature macroporous hydroxyapatite scaffolds by foaming and hydrolysis of an α-TCP paste." Biomaterials, 25, 3671-3680, 2004.

3. Aro HT, Chao EYS, Day SM, Einhorn TA, Ostrum RF, Rubin CT: "Bone injury, regeneration, and repair." Chapter 14 Orthopaedic Basic Science: American Academy of Orthopaedic Surgeons.

4. Bao QB, McCullen GM, Higham PA, Dumbleton JH, Yuan HA: "The artificial disc: theory, design and materials." Biomaterials, 17, 1157-1167, 1996.

5. Boskey A, Bostrom MPG, Einhorn TA, Kaufman JK: "Form and function of bone." Chapter 13 Orthopaedic Basic Science: American Academy of Orthopaedic Surgeons.

6. Brown TD, Heiner AD: "Structural properties of a new design of composite replicate femurs and tibias." Journal of Biomechanics, 34, 773-781, 2001.

7. Bushell GR, Ghosh P, Taylor TF, Akeson WH: Proteoglycan chemistry of the intervertebral disks. Clinical Orthopedics,115-123, 1977.

8. Chang BS, Lee CK, Hong KS, Youn HJ, Ryu HS, Chung SS, Park KW: "Osteoconduction at porous hydroxyapatite with various pore configurations." Biomaterials, 21,12, pp 1291-1298, 2000.

9. Cornell CN, Lane JM: "Current Understanding of Osteoconduction in Bone Regeneration." Clinical Orthopaedics and Related Research, 1(355S), S267-S273, October 1998.

10. Crock HV, Yoshizawa H: The blood supply of the lumbar vertebral column. Clinical Orthopedics, 6-21, 1976.

11. Dreyer SJ, Dreyfuss PH: Low back pain and the zygapophysial (facet) joints. Archives in Physical Medicine and Rehabilitation, 77, 290-300, 1996.

12. Dunlop RB, Adams MA, Hutton WC: "Disc space narrowing and the lumbar facet joints." J Bone Joint Surg Br, 66, 706-710, 1984.

13. Harris LD, Kim BS, Mooney DJ: "Open pore biodegradable matrices formed with gas foaming." Journal of Biomedical Materials Research, 42, pp 396-402, 1998.

14. http://faculty.uscs.edu/llever/Polymer%20Resources/Synthesis.htm#chain

15. http://herkules.oulu.fi/isbn9514271246/html/x485.html

16. Humzah MD, Soames RW: Human intervertebral disc: structure and function. Anatomy Rec, 220, 337-356, 1988.

17. Jasty, Morali. "In Vivo Skeletal Responses to Porous-Surfaced Implants Subjected to Small Induced Motions." The Journal of Bone and Joint Surgery, 79-A(5), 707-714, 1997.

18. Kaw AK. Mechanics of Composite Materials. CRC press, Boca Raton, 1997.

19. Kiefer J, Hilborn JG, Hiedrick JL: "Chemically induced phase separation: a new technique for the synthesis of macroporous epoxy networks." Polymer, 37, 25, 5715-5725.

20. Kiefer J, Hilborn JG, Manson JAE, Leterrier Y: "Macroporous epoxy networks via chemically induced phase separation." Macromolecules, 29, 4158-4160, 1996.

21. Kokubo T, Kim HM, Kawashita M: "Novel bioactive materials with different mechanical properties." Biomaterials, 24, pp 2161-2175, 2003.

22. Kuslich SD: Lumbar degenerative disc disease-axial back pain: posterior approach, in Vaccaro AR, Albert TJ (eds): Mastercases: Spine Surgery. New York, Thieme, 2001, 84-92.

23. LeGeros RZ: "Properties of osteoconductive biomaterials: calcium phosphates." Clinical Orthopedics, 395, 81-98, 2002.

24. Lewandowska-Szumiel M, Komender J, Chlopek J: "Interaction between carbon composites and bone after intrabone implantation." Journal of Biomedical Materials Research, 48, 3, 289-296, 1999.

25. Liao CJ, Chen CF, Chen JH, Chiang SF, Lin YJ, Chang KY: "Fabrication of porous biodegradable polymer scaffolds using a solvent merging/particulate leaching method." Journal of Biomedical Materials Research, 59, 676-681, 2002.

26. Loera AG, Dumon M, Pascault JP: "Porous epoxy thermosetting polymers obtained by a phase separation process in the presence of emulsifiers." Macromolecular Symposia, 151, 341-346, 2000.

27. Marieb, Elaine N. Human Anatomy & Physiology Fourth Edition. Benjamin/Cummings Press, 1998.

28. Martin RB, Burr DB, Sharkey NA. Skeletal Tissue Mechanics. Springer-Verlag, New York, 1998.

29. Mikos AG, Temenoff JS: "Formation of highly porous biodegradable scaffolds for tissue engineering." Electronic Journal of Biotechnology, 3, 2, 2000.

30. Nam YS, Yoon JJ, Park TG: "A Novel Fabrication Method of Macroporous Biodegradable Polymer Scaffolds Using Gas Foaming Salt as a Porogen Additive." Journal of Biomedical Materials Research: 53, 1-7, 2000.

31. Panjabi M, White A. Clinical Biomechanics of the Spine Second Edition. Philadelphia, Lippincott, 1990.

32. Piconi C, Maccaurro G: "Zirconia as a ceramic biomaterial." Biomaterials, 20, 1-25, 1999.

33. Oh SH, Kang SG, Kim ES, Cho SH, Lee JH: "Fabrication and characterization of hydrophilic poly(lactic-co-glycolic acid)/ poly(vinyl alcohol) blend cell scaffolds by melt-molding particulate-leaching method." Biomaterials, 24, 4011-4021, 2003.

34. Ramay HR, Zhang M: "Preparation of porous hydroxyapatite scaffolds by combination of the gel-casting and polymer sponge methods." Biomaterials, 24, 3293-3302, 2003.

35. Ratner BD, Hoffman AS, Schoen FJ, Lemons JE. Biomaterials Science. Academic Press, 1996.

36. Sideridis E, Papadopoulos GA: "Short-beam and three-point-bending tests for the study of shear and flexural properties in unidirectional-fiber-reinforced epoxy composites." Journal of Applied Polymer Science, 93, 63-74, 2004.

37. Shastri VP, Martin I, Langer R: "Macroporous polymer foams by hydrocarbon templating." Proceedings of the National Academy of Sciences USA. February 29; 97(5): 1970-1975, 2000.

38. Stefani PM, Barchi AT, Sabugal J, Vazquez A: "Characterization of epoxy foams." Journal of Applied Polymer Science, 90, 11, 2992-2996, 2003.

39. Tadic D, Beckmann F, Schwarz K, Epple M: "A novel method to produce hydroxyapatite objects with interconnecting porosity that avoids sintering." Biomaterials, 25, 3335-3340, 2004.

40. Vaccaro AR: "The role of the osteoconductive scaffold in synthetic bone graft." Orthopedics, May 2002 supplement.

41. Whang K, Thomas CH, Healy KE: "A novel method to fabricate bioabsorbable scaffolds." Polymer, 36, 4, 837-842, 1995.

42. Yildirim OS, Aksakal B, Celik H, Vangolu Y, Okur A: "An investigation of the effects of hydroxyapatite coatings on the fixation strength of cortical screws." Medical Engineering Physics, 27, 3, 221-228, 2005.

43. Yong-Hing K, Kirkaldy-Willis WH: The three-joint complex, in Weinstein JN, Wiesel SW (eds): The Lumbar Spine, Philadelphia, Saunders, 1990, 80-87.

44. Yoon JJ, Park TG: "Degradation behaviors of biodegradable macroporous scaffolds prepared by a gas foaming of effervescent salts." Journal of Biomedical Materials Research, 55, 401-408, 2000.

45. Yoon JJ, Kim JH, Park TG: "Dexamethasone-releasing biodegradable polymer scaffolds fabricated by a gas-foaming/salt-leaching method." Biomaterials, 24, 2323-2329, 2003.

46. Zhang XS, Evans SL, Gregson PJ: "In vivo biocompatibility and mechanical study of novel bone-bioactive materials for prosthetic implantation." Journal of Biomedical Materials Research, 46, 2, 279-286, 1999.

47. Zhao JL, Fu T, Han Y, Xu KW: "Reinforcing hydroxyapatite/thermosetting epoxy composite with 3-D carbon fiber fabric through RTM processing." Materials Letters, 58, 163-168, 2003.

48. Zoltek: User's Guide to Short Carbon Fiber Composites. Zoltek Companies, St. Louis, MO, June 2000.